Concentric zones, cell migration and neuronal circuits in the Drosophila visual center

メタデータ	言語: eng 出版者: 公開日: 2017-10-06 キーワード (Ja): キーワード (En): 作成者: メールアドレス: 所属:
URL	https://doi.org/10.24517/00039999

This work is licensed under a Creative Commons Attribution-NonCommercial-ShareAlike 3.0 International License.

Concentric zones, cell migration and neuronal circuits in the *Drosophila* visual center

Eri Hasegawa[1,6], Yusuke Kitada[1,2,3,6] Masako Kaido[1], Rie Takayama[1], Takeshi Awasaki[4], Tetsuya Tabata[3] and Makoto Sato[1,5,*]

[1]Frontier Science Organization, Kanazawa University, 13-1 Takaramachi Kanazawa-shi, Ishikawa 920-8641, Japan. [2]Graduate Program in Biophysics and Biochemistry, Graduate School of Science, University of Tokyo, 7-3-1 Hongo, Bunkyo-Ku, Tokyo 113-0033, Japan. [3]Institute of Molecular and Cellular Biosciences, University of Tokyo, 1-1-1 Yayoi, Bunkyo-ku, Tokyo 113-0032, Japan. [4]University of Massachusetts Medical School, USA. [5]PRESTO, JST, 4-1-8 Honcho Kawaguchi, Saitama 332-0012, Japan. [6]These authors contributed equally to this work

*Correspondence: makotos@staff.kanazawa-u.ac.jp

Summary

A wide variety of neurons comprise the *Drosophila* optic lobe, forming laminar

neuropiles with columnar units and topographic projections from the retina. The *Drosophila* optic lobe shares many structural characteristics with mammalian visual systems. However, little is known regarding the developmental mechanisms that produce neuronal diversity and organize the circuits in the primary region of the optic lobe, the medulla.

Here, we describe the key features of the developing medulla and report novel phenomena that could accelerate our understanding of the *Drosophila* visual system. The identities of medulla neurons are pre-determined in the larval medulla primordium, which is subdivided into concentric zones characterized by the expression of four transcription factors: Drifter, Runt, Homothorax and Brain-specific-homeobox (Bsh). The expression pattern of these factors correlates with the order of neuron production. Once the concentric zones are specified, the distribution of medulla neurons changes rapidly. Each type of medulla neuron exhibits an extensive but defined pattern of migration during pupal development. The results of clonal analysis suggest *homothorax* is required to specify the neuronal type by regulating various targets including Bsh and cell adhesion molecules such as N-cadherin, while *drifter* regulates a subset of

morphological features of Drifter-positive neurons. Thus, genes that show the concentric zones may form a genetic hierarchy to establish neuronal circuits in the medulla.

Introduction

In many animals, visual information is processed by visual centers in the brain that are composed of laminar structures and columnar units with topographic input from the retina. The neuronal circuits in the visual centers process various types of visual information such as motion, color and shape. As noted by Cajal, the fly optic lobe shares structural characteristics with mammalian visual systems (Sanes and Zipursky, 2010), and *Drosophila* genetics allow high resolution genetic manipulations (Gao et al., 2008; Rister et al., 2007). The *Drosophila* visual system may provide a powerful model to investigate the mechanisms underlying the formation of visual processing circuits. However, little is known regarding the developmental processes that create neuronal diversity and organize these circuits in the primary region of the optic lobe, the medulla.

The *Drosophila* retina is composed of ~800 ommatidial units, each containing

eight types of photoreceptor neurons (R1-8). R1-6 detect moving stimuli (Katsov and Clandinin, 2008; Rister et al., 2007; Zhu et al., 2009), while R7-8 are involved in color vision (Gao et al., 2008; Morante and Desplan, 2008). Visual information received in the retina is transmitted to the optic lobe composed of lamina, medulla, lobula and lobula plate. The medulla, lobula and lobula plate are subdivided into ten (M1-10), six (Lo1-6) and four (Lop1-4) strata, respectively.

The medulla is the largest component of the *Drosophila* optic lobe, containing approximately 40,000 neurons forming 10 layers. In Golgi studies, 60 types of medulla neurons with different morphological characteristics have been identified (Fischbach and Dittrich, 1989; Hofbauer and Campos-Ortega, 1990). Because R7-8 axons terminate in the medulla and the visual information carried by R1-6 axons is sent to the medulla through a relay by lamina neurons, the medulla might process all of the visual information received in the retina (Takemura et al., 2008). In spite of the medulla's importance, the developmental mechanisms that produce neuronal diversity and organize medulla circuits remain largely unknown. In the larval brain, the primary source of medulla neurons is thought to be neuroblasts (NBs) situated in the outer

proliferation center (OPC; Hofbauer and Campos-Ortega, 1990; Yasugi et al., 2008). The differentiation of NBs from neuroepithelial cells (NEs) progresses from the medial to the lateral region of the OPC, and each NB produces ganglion mother cells (GMCs) that subsequently divide to become neurons (Egger et al., 2007; Toriya et al., 2006). A key goal in developmental neurobiology is understanding the molecular mechanisms by which each of 40,000 neurons in the medulla establishes an appropriate identity among 60 different possibilities and connects to appropriate targets to form neuronal circuits.

Here, we describe the key features of the developing medulla and report novel observations that could accelerate our understanding of the *Drosophila* visual system. During larval development, the medulla is subdivided into concentric zones that are characterized by the expression of four conserved transcription factors: Drifter (Drf), Runt (Run), Homothorax (Hth) and Brain-specific-homeobox (Bsh)(Anderson et al., 1995; Gergen and Butler, 1988; Jones and McGinnis, 1993; Kurant et al., 1998; Pai et al., 1998; Rieckhof et al., 1997). The expression patterns of these factors correlate with the order of neuron production. Once the concentric zones are specified, the distribution of medulla neurons changes rapidly, and the concentric zones are disrupted early in

pupal development due to the extensive migration of cell bodies. The projection patterns of medulla neurons are established through a series of steps—axonal projection, cell body migration and dendritic arborization—that are stereotypically defined according to the neuronal type most likely governed by genes that show the concentric zones.

Materials and methods

Generation of Gal4 strains

Following DNA fragments were PCR amplified using primers listed in Table S1.

***drf-Gal4*:** The drfL, Gal4 and drfR fragments were inserted to *pW25* to have *drfGal/W25*, which was used for homologous recombination (Gong and Golic, 2003). Although drfR was precisely inserted into the *drf* locus as revealed by PCR, drfL was not. Since Drf expression was detected in *drf-Gal4* homozygous clones, it does not eliminate the *drf* ORF (not shown).

***hth-Gal4*:** The hthL, Gal4 and hthR fragments were inserted to *pW25* to have *hthGal/W25*, which was introduced to the *hth* locus by converting to the *hth-lacZ* insertion using *Δ2-3* (Sepp and Auld, 1999). *hth-Gal4* was inserted between exons 9-10.

Hth expression was significantly reduced in *hth-Gal4* homozygous clones (not shown).

***bsh-Gal4*:** The bshLz, Gal4, Kmr and bshRz fragments were inserted to *pW25* to have *bshLRzGal4Kmr*, which was inserted to a BAC containing the *bsh* locus (Kimura et al., 2006; Venken et al., 2006). The bshLB and bshRB fragments at the boundary of the *bsh* locus were inserted to *attB-Pacman-ApR*. The *bsh* locus was retrieved from the BAC to obtain *bshGalBAC/Pacman*, which was introduced to the fly genome by P-element mediated transformation (third chromosome).

Fly Strains

repo-Gal4, AyGal4, Actin>stop>lacZ, UAS>CD2>CD8GFP, UAS-flp, hs-flp, elav-Gal4, UAS-CD8GFP, tub-Gal80, FRT40A, FRT2A, FRT82B, M(3R)w, UAS-GFP, UAS-nlsGFP, UAS-SytHA, UAS-tau-myc, drf^{E82}, drf^{H76}, UAS-drf, hth^{P2}, UAS-hth, hth-lacZ, $NCad^{M19}$, $NCad^{omb405}$, NP2646 (*CG11873*) and *NP6013* (*amnesiac*). *dpn-Gal4* (provided by Ethan Bier).

Clonal analysis

Following genetic crosses and heat shock conditions were used.

Fig. 2: *hs-flp*; *UAS-CD8GFP* was crossed to *AyGal4* (32ºC 15 minutes at early 3rd instar, dissected 36 hours after heat shock).

Fig. 3: *elav-Gal4 UAS-CD8GFP hs-flp*; *tub-Gal80 FRT2A* was crossed to *FRT2A* (37ºC 60 minutes at 2nd instar).

Fig. 4: *hs-flp*; *UAS>CD2>CD8GFP* was crossed to *hth-Gal4*, *NP6013* and *bsh-Gal4* flies. *hs-flp*; *FRT82B tub-Gal80* was crossed to *UAS-SytHA*; *FRT82B bsh-Gal4 UAS-CD8GFP* (32-33ºC 60 minutes at 3rd instar).

Fig. 5: y^+ *FRT40A*; *hth-Gal4 UAS-CD8GFP* was crossed to *hs-flp*; *tub-Gal80 FRT40A*; *UAS-CD8GFP*. *hs-flp*; *FRT82B tub-Gal80* was crossed to *FRT82B hth-Gal4 UAS-CD8GFP*. *hs-flp*; *UAS-hth*; *FRT82B tub-Gal80* was crossed to *FRT82B hth-Gal4 UAS-CD8GFP* (32-33ºC 60 minutes at 3rd instar). *hs-flp*; *FRT82B tub-Gal80* was crossed to *FRT82B bsh-Gal4 UAS-CD8GFP* or *FRT82B bsh-Gal4 UAS-CD8GFP* hth^{P2}. *hs-flp*; *UAS-hth*; *FRT82B tub-Gal80* was crossed to *FRT82B bsh-Gal4 UAS-CD8GFP* hth^{P2} (32-35ºC 60 minutes at 3rd instar). *hs-flp*; *tub-Gal80 FRT40A*; *UAS-CD8GFP* was crossed to *NP6013*; $NCad^{M19\ or\ omb405}$ *FRT40A*; *UAS-CD8GFP* or *NP6013*; y^+ *FRT40A*;

UAS-CD8GFP (32ºC 60 minutes at 2nd to early 3rd instar). *hs-flp*; *tub-Gal80 FRT40A*; *UAS-CD8GFP* was crossed to *NCad*$^{M19\ or\ omb405}$ *FRT40A*; *bsh-Gal4 UAS-CD8GFP* or y^{+} *FRT40A*; *bsh-Gal4 UAS-CD8GFP* (32-33ºC 60 minutes at 3rd instar). *hs-flp*; *AyGal4 UAS-GFP* was crossed to *UAS-hth* (34ºC 30-60 minutes at early 3rd instar). *hs-flp*; *FRT82B hth*^{P2} was crossed to *FRT82B ubi-GFP M(3R)w* flies (37ºC 60 minutes at 1st instar).

Fig. 6: *hs-flp*; *tub-Gal80 FRT40A*; *drf-Gal4 UAS-CD8GFP* was crossed to *UAS-SytHA*; *FRT40A* flies (31ºC 30 minutes at 3rd instar).

Fig. 7: *UAS-SytHA*; *tub-Gal80 FRT2A* was crossed to *hs-flp*; *FRT2A UAS-CD8GFP NP2646* or *hs-flp; drf*$^{E82\ or\ H76}$ *FRT2A UAS-CD8GFP NP2646*. *hs-flp*; *UAS-drf*; *tub-Gal80 FRT2A* was crossed to *hs-flp*; *drf*^{E82} *FRT2A UAS-CD8GFP NP2646* (33ºC 20 minutes at 3rd instar).

Histochemistry

rabbit anti-Hth (Adi Salzberg, 1:1000), guinea pig anti-Bsh (Chi-Hon Lee, 1:500), guinea pig anti-Run (Asian Distribution Center, 1:500), rat anti-Drf (Sarah Certel,

1:3000), guinea pig anti-Dpn (James Skeath, 1:1000), mouse anti-HA (Covance, 1:1000), mouse anti-lacZ (Promega, 1:250), rat anti-CD8 Alexa488 conjugated (Caltag, 1:100) and rabbit anti-GFP Alexa488 conjugated (Invitrogen, 1:2000). mouse anti-Chaoptin (1:10), mouse anti-ChAT (1:300), mouse anti-Cut (1:20), mouse anti-Dac (1:20), rat anti-Elav (1:100), mouse anti-Myc (1:20), rat anti-NCad (1:20), mouse anti-Pros (1:10) and mouse anti-Repo (1:10) from DSHB. Custom-made antibodies (rabbit anti-Hth, guinea pig and rat anti-Bsh, Run, Drf antibodies) were raised as described (Jones and McGinnis, 1993; Kosman et al., 1998; Kurant et al., 1998; Llimargas and Casanova, 1997). Details are available upon request. *in situ* hybridization was performed as described (Sato et al., 2006). Images were processed using Zeiss LSM image browser, Adobe Photoshop and Bitplane Imaris.

Results

The larval medulla is subdivided into concentric zones expressing conserved transcription factors

To identify genetic subdivisions in the medulla primordium of the larval brain, the

expression of conserved transcription factors was examined. We identified concentric zones characterized by the expression of four conserved genes that encode transcription factors: Drifter (Drf) from the Brn family, Runt (Run) from the Runx family, Homothorax (Hth) from the Meis family and Brain-specific-homeobox (Bsh) from the Bsx family (Fig. 1D,E; Anderson et al., 1995; Gergen and Butler, 1988; Jones and McGinnis, 1993; Rieckhof et al., 1997). All of these genes, which we collectively call ‘concentric genes’, were expressed in differentiated neurons (Fig. 1F); however, weak Hth signals were also found in NBs and NEs (Fig. 1D’,E’). The concentric zones expressing Drf, Run and Hth were adjacent but did not overlap (Fig. 1D). Bsh expression was found in the outer sub-domain of the Hth domain (Fig. 1E). Medulla neurons projected axon-like structures toward the center of the brain hemisphere to form concentric neuropiles (Fig. 1A,B,F). Accumulations of tau-Myc suggest that the axon-like structures are indeed axons (Fig. 1J; Thor et al., 1999). Large glial cells were found on the surface of the medulla, while small glial cells were in the innermost area of the medulla cortex adjacent to the Hth domain (Fig. 1G), which most likely become the medulla neuropile glia (MNG; see Fig. 3B; Tix et al., 1997). The processes of glial cells

were found in the larval medulla cortex (Fig. 1G).

The birth order of medulla neurons correlates with concentric gene expression

The NBs are formed from NEs in the OPC during early third larval instar. NB produces GMCs that subsequently divide to produce medulla neurons (Colonques et al., 2007; Egger et al., 2007; Nassif et al., 2003; Toriya et al., 2006; Yasugi et al., 2008). Many neurons are produced from a single NB with a linear and radial orientation toward the center of the developing medulla (Fig. 1A,B). A weak expression of concentric genes appeared around mid third instar (not shown).

Each clone of neurons produced from a single NB formed a line that intersected the concentric zones (Fig. 1A,B,H,I); thus, the expression of concentric genes may not be lineage-dependent. Each NB may produce several types of medulla neurons that are distinguished by the expression of concentric genes. To address this possibility, a small group of cells were labeled with constitutive expression of *UAS-CD8GFP* (Fig. 2A,B; Ito et al., 1997). Mild induction of FLPase triggered GFP expression in a single NB, as identified by Deadpan (Dpn) expression, and in daughter cells of the NB (Fig. 2B; Bier

et al., 1992). The GFP-positive neurons are thus thought to derive from a single NB. Our observations suggest that various combinations of neurons can be produced from a single NB (Drf/Bsh, Drf/Run, Bsh/Hth, Run/Hth; Fig. 2B and not shown). Because we could not restrict the timing of clone induction in newborn NBs, a subset of daughter cells produced from a NB could be labeled with GFP. However, a single NB clone tended to contain 2-3 Drf-positive, one Run-positive and one Bsh-positive neurons (Fig. 2C), suggesting that many of the NBs have essentially the same potential to produce a series of medulla neurons (Fig. 2D).

Because NBs produce neurons directed toward the center of the medulla, it is likely that neurons born early in development are located in inner concentric zones while late-born neurons are found in outer zones. To confirm this theory, we utilized a neuroblast specific Gal4 driver (*dpn-Gal4*) that specifically expresses *Gal4* mRNA in NB cells (Fig. 2G,H). Differentiated neurons inherit the Gal4 protein even after *Gal4* transcription is terminated; thus, a strong GFP signal was detected in neurons in the outer concentric zones (Fig. 2E). However, the GFP signal was decreased in neurons distant from NBs and was not detectable in the innermost zones. A prominent GFP

signal was observed in the innermost, non-neuronal glial cells (Fig. 2F), a result supporting the hypothesis that NBs produce glial cells that subsequently migrate toward the medulla neuropile (Colonques et al., 2007). The signal intensity of GFP roughly correlated with concentric gene expression; strong GFP expression was found in Drf-positive neurons but gradually decreased in Run and Bsh-positive zones (Fig. 1D',2E,I). These results are consistent with the idea that the birth order of medulla neurons may control neuronal type via concentric gene expression.

Medulla neurons migrate extensively and the concentric zones are disrupted during pupal development

The expression of concentric genes in the larval medulla primordium may regulate neuronal identities and contribute to the formation of neuronal circuits in the adult medulla. We thus examined concentric gene expression during pupal development (Fig. 3A). The concentric zones found in the larval medulla were essentially conserved during early pupal development until 8 hours after puparium formation (APF; Fig. 3A1). However, the concentric zones began to collapse at 12 hours APF (Fig. 3A2). The

distribution of neurons continued to change until 24 hours APF, becoming completely disorganized (Fig. 3A3-5). The same disorganized pattern was found in the adult brain (Fig. 3A6). Because the expression of concentric transcription factors appeared stable and strong, it is likely that cell bodies migrate extensively between 12 and 24 hours APF without changing gene expression. Hth- and Drf-positive cells were found in the innermost and outer zones of the larval medulla, respectively. However, both Hth- and Drf-positive cells were found in the inner and outer zones in adults (Fig. 3A6). This result suggests that the cell bodies of medulla neurons may be migrating in a radial pattern.

In order to address if they are indeed migrating, clones of medulla neurons were constitutively labeled with GFP (Lee and Luo, 1999). The relative distributions of GFP-positive cells before and after migration were compared (Fig. 3C). Because the NBs situated in the outermost region of the larval medulla primordium produce neurons with a radial orientation, GFP-positive neurons were linearly arranged in the larval brain (Fig. 3C1). Similar distributions of GFP positive cells were found at the beginning of migration at 12 hours APF (Fig. 3C2). However, after the completion of migration at 24

hours APF, GFP positive cells were stochastically distributed (Fig. 3C3). Therefore, medulla neurons changed their relative locations between 12 and 24 hours APF. Because a radial migration would not disrupt the radial arrangement of cells, medulla neurons may also migrate with a tangential orientation, perpendicular to the linear arrangement of GFP-positive cells in the larval brain (Fig. 3C1).

To determine whether the expression of concentric genes persists during metamorphosis, Drf-positive neurons were constitutively labeled with LacZ (Fig. S1). A Gal4 driver that accurately mimics *drf* expression (*drf-Gal4*) was used to express FLPase to constitutively label Drf-positive cells with LacZ (Fig. S1; McGuire et al., 2003; Struhl and Basler, 1993). If *drf* expression persists during metamorphosis, all of the LacZ positive neurons in the adult brain should express GFP, which is under the control of *drf-Gal4*. Indeed, our data suggest that *drf* expression persists during metamorphosis.

Changes in distributions of Hth-, Run- and Drf-positive neurons were seemingly random. However, Bsh/Hth double positive neurons displayed a clear pattern of migration (Fig. 3B). Because Bsh is expressed in a subset of Hth-positive neurons,

Bsh/Hth-positive cells were initially situated in the inner area of the medulla primordium (Fig. 1E,3B1). However, they always moved outward during metamorphosis and were eventually situated in the outermost area of the adult medulla (Fig. 3B2-6). This finding suggests that the migration of medulla neurons is indeed an organized and patterned process, but that labeling several types of neurons may obscure the migration pattern. Because the projection pattern of Bsh/Hth-positive neurons could be continuously traced from the larval to adult medulla (Fig. 5), we assume that the expression of Bsh and Hth in these neurons does not change throughout development. The locations of Drf-positive neurons in the adult brain could also be classified according to neuronal subtypes (Fig. S4), again suggesting that each type of medulla neuron exhibits a stereotyped migration pattern.

Hth is expressed in four types of medulla neurons, while co-expression of Hth and Bsh is found in a single subtype

To investigate projection patterns of Hth-positive neurons, a Gal4 driver that mimics *hth* expression was generated (Materials and Methods). The resulting *hth-Gal4* allele widely

induced *UAS-GFP* expression in the larval medulla probably due to residual expression of Gal4 produced in NBs. In the adult brain, *hth-Gal4* largely recapitulated Hth expression (Fig. 4A). We also searched for Gal4 drivers that mimic Hth expression. *NP6013* induced *UAS-CD8GFP* expression in a subset of Hth-positive neurons in the larval brain (Fig. 4B). The projections of Hth-positive medulla neurons were already present in the larval brain; their terminals were restricted to the medulla neuropile and were not found in the lobula complex (lobula and lobula plate; Fig. 4B).

Generating single cell clones expressing *CD8GFP* under the control of *hth-Gal4* and *NP6013* (Wong et al., 2002), we identified at least four types of Hth-positive neurons in the adult brain (Fig. 4C-F,S2B). As observed in the larval medulla, none of these neurons projected to the lobula complex (Fig. 4B). Neuronal types were classified according to the combinations of layers to which they project, as confirmed by N-Cadherin expression (NCad; Fig. 6E3; Fischbach and Dittrich, 1989; Morante and Desplan, 2008). The neuronal type most frequently oberved was Mi1, which shows small arborizations at M1, M5 and M9-10 (Fig. 4C,S2B). Neurons that show stratifications at M1 and M4 in the medulla and projections to the lamina were

temporalily named lamina wide field-like1 (Lawfl1; Fig. 4D; Fischbach and Dittrich, 1989) since arborizations in the lamina were barely detectable due to weak GFP expression. The other Lawf-like neuron, Lawfl2, showed arborizations at M1 and M8-10 in the medulla and projections to the lamina (Fig. 4E). Lawfl2 has not been described in the literature. Pm3 are local neurons restricted to the proximal medulla (Fig. 4F).

Bsh is expressed in a subset of Hth-positive neurons from larval to adult stages (Fig. 1E,3B). We found that Bsh was only expressed in Mi1 type neurons in the adult medulla (Fig. S2B). We thus generated a *bsh-Gal4* strain by inserting the *Gal4* coding sequence into the genomic fragment of the *bsh* gene that contains the entire *bsh* locus (Materials and Methods). The expression of *bsh-Gal4* was similar to Bsh in adults (Fig. 4G). Indeed, mosaic analyses using *bsh-Gal4* specifically indicated the presence of Mi1 neurons in the medulla. Presynaptic sites were revealed using synaptotagmin-HA (SytHA; Robinson et al., 2002). The SytHA signal was very strong at M9-10 but weak or hardly detectable at M1/5, suggesting that Mi1 neurons have postsynaptic sites at M1/5 and a presynaptic site at M9-10 shaped like a fish hook (Fig. 4H).

In addition to the morphological features, neurotransmitters are important characteristics of neurons. We found that choline acetyltransferase (ChAT) was always up-regulated in Bsh-positive neurons in adults (Fig. 4I). Therefore, Bsh expression alone can identify a specific type of medulla neuron, Mi1, which stereotypically migrates outward during metamorphosis and is cholinergic.

Hth regulates Bsh expression and neuronal identities

The roles of *hth* in medulla neuron formation were examined by generating *hth-Gal4*-homozygous mutant clones and visualizing their neuronal projection patterns (Fig. 5). The loss of *hth* function completely changed the morphology of *hth-Gal4*-positive medulla neurons, making cells apparently switch neuronal types (Fig. 5,S3A). In a *hth-Gal4*-heterozygous background, control clones exhibited the normal morphology of Hth-positive neurons, primarily Mi1 (Fig. 5D). In *hth-Gal4*-homozygous clones, normal Mi1 neurons were not found; instead, we frequently observed neurons very different from Mi1, neurons that were Hth-negative on a wild-type background such as Tm13-like and other Tm-type lobula projection neurons (Fig. 5B,D,S3A).

Mi1-like abnormal neurons, which were similar to Mi1 but exhibited irregular arborizations, were occasionally found (Fig. 5A,D). The fish hook-like shape at M9-10 was occasionally disrupted in the Mi1-like abnormal neurons. The phenotype could partially be rescued by introducing exogenous *hth* (Fig. 5D,S3A). Thus, the loss of *hth* function transforms Hth-positive neurons into diverse types of medulla neurons that are likely specified by genes other than *hth*.

Using *bsh*-Gal4, consistent phenotypes were observed in clones homozygous for a strong hypomorphic allele, hth^{P2}. In control experiments, *bsh-Gal4* exclusively labeled Mi1 neurons (Fig. 5D). However, Tm1-like rather than Mi1 neurons were found in hth^{P2}-homozygous clones (Fig. 5C,D,S3A). The formation of Mi1 was partially rescued by introducing exogenous *hth* (Fig. 5D,S3A). In contrast to the distal localization of Mi1 cell bodies in the wild-type medulla cortex, the cell bodies of *hth*-mutant Tm-like neurons were found in the proximal to intermediate cortical zone (n=11/16; Fig. 5C). Therefore, *hth* is essential to determining the identity of Mi1 neurons, including the location of cell bodies in the adult brain. Cell bodies of non-Mi1 type Hth-positive neurons tended to be found in more proximal cortical zones in the wild-type medulla

cortex (Fig. 3B6). Thus, *hth* and *bsh* may co-operate to determine the location of Mi1 cell bodies.

Because Hth was weakly expressed in NE and NB cells in the larval brain (Fig. 1D',E'), the *hth*-mutant phenotypes shown above may be caused by general defects in neurogenesis resulting from abnormalities in neuronal precursor cells. However, we did not detect such defects in production of GMCs and neurons, as determined by Prospero and Elav expression in *hth*-mutant clones in the larval medulla (Fig. S3B).

Hth may regulate expression of downstream target genes to control specification and formation of Hth-positive neurons. *bsh* is a potential candidate of Hth-target gene because Bsh expression was frequently reduced in *hth* mutant clones (Fig. 5L). However, residual Bsh expression was detected (Fig. 5L). This may be due to hypomorphic nature of hth^{P2}, or *hth* function may not be essential for Bsh expression (e.g. *hth* and an unidentified gene may act partially redundantly). Interestingly, the transformation of Mi1 neurons to Tm1-like neurons, as revealed by *bsh-Gal4*, was observed in both Bsh-positive (n=4/65) and Bsh-negative (n=61/65) clones that were *hth* mutants. In most cases, Mi1-like abnormal neurons were positive for Bsh (n=7/8),

suggesting that Bsh expression alone cannot determine the fate and morphology of Mi1 neurons.

NCad may act downstream of Hth to regulate projection of Mi1 neurons

The development of Mi1 neurons was traced from the larval to adult brain using *NP6013* and *bsh-Gal4* (Fig. 5E-H). At the end of larval development (0 hours APF), Bsh-positive neurons form two arborization sites along the neuropile structures strongly expressing NCad (proximal and distal NCad domains; Fig. 5E). Found in the proximal NCad domain, the arborization at the tip of axonal shafts most likely corresponds to the terminal at M9-10 in adults (Fig. 4H,5H). In the distal NCad domain, the third arborization site, which most likely becomes M1 arborization in adults, was occasionally found immediately distal to the pre-existing M5 arborization at 24 hours APF (Fig. 5G). At 20 hours APF, typical Mi1 neurons lacked the third arborization while cell bodies were located in the distal cortical area, suggesting that the M1 arborization is formed around 20-24 hours APF coincidently with the completion of cell body migration (Fig. 5F,G).

While NCad was widely expressed in the cell bodies of larval medulla neurons, its expression was up-regulated in the Hth-positive, innermost concentric zone (Fig. 5J). Because NCad was ectopically up-regulated in *hth*-expressing clones and was autonomously reduced to the basal level in *hth* mutant clones (Fig. 5K,L), NCad up-regulation is most likely controlled by *hth* in the larval brain. NCad is a homophilic cell adhesion molecule; therefore, neurites of Mi1 neurons that strongly express NCad may innervate targets also expressing high levels of NCad (Iwai et al., 1997). NCad is known to regulate the target layer specificity of R-axons and lamina neurons (Lee et al., 2001; Nern et al., 2008; Ting et al., 2005). Thus, NCad up-regulation in Mi1 may influence the arborization sites of Mi1 neurons located in the proximal and distal NCad domains in the larval medulla neuropile (Fig. 5E,J). Only the proximal arborizations were occasionally eliminated in clones homozygous for $NCad^{M19}$ (n=6/10; Fig. 5I) and $NCad^{omb405}$ (n=3/6; not shown). The defects found in the adult brain were diverse and may not specifically derive from larval defects. However, the loss of or disorganized M9-10 terminals can be explained by a lack of NCad up-regulation in Mi1 neurons during larval development (Fig. 5I and not shown).

Drf is expressed in nine types of medulla neurons

To compare neuronal types of Drf- and Hth-positive population, we generated *drf-Gal4* strains that accurately mimic *drf* expression (Materials and Methods). The *drf-Gal4* induced GFP expression in a manner identical to Drf distribution throughout development (Fig. 6A,B). In the adult medulla, restricted subsets of medulla strata were densely labeled with GFP (Fig. 6E). In the lobula, axonal terminals were exclusively found in layers Lo1 and Lo4. Drf-positive neurons thus project to common target layers in the adult lobula.

To identify neuronal types showing Drf expression, we performed MARCM analyses using *drf-Gal4* to catalog Drf-positive medulla neurons in adults and identified nine subtypes of Drf-positive neurons (Fig. 6F-M), the majority of which were lobula projection neurons that projected to the lobula complex (TmY3, Tm27(Y), Tm9 and Tm3; Fig. 6F-J). In the distal medulla, SytHA was weak or hardly detectable, but was prominent in the lobula complex. Thus, the arborizations in the distal medulla were primarily postsynaptic while terminals in the lobula complex were presynaptic. We also

identified three types of local neurons (Mi10b, Dm8a and Dm8b; Dm8a is similar to Dm8 in the literature) whose innervations were restricted to the medulla (Fig. 6K-M). A stochastic distribution of SytHA was found along arborizations of these local neurons. Tm27 and Tm27Y neurons have not been previously described. Tm3b neurons are similar to Tm3 neurons (hereafter Tm3a) with the exception of a small branch at M10 projecting back toward M8 (Fig. 6J).

The Bsh/Hth-positive Mi1 neurons were shown to stereotypically migrate from the inner to outer areas of the medulla cortex (Fig. 3B). To determine whether a similar migration pattern occurs in Drf-positive neurons, locations of cell bodies in the medulla cortex were categorized into distal, intermediate and proximal zones (Fig. S4). For each subtype of Drf-positive neurons, locations of cell bodies were examined. As a result, we found that four subtypes of Drf neurons have cell bodies in the distal zone; three subtypes in the intermediate zone and two subtypes in the proximal to intermediate zones. Thus, cell body location correlated with the neuronal subtype of Drf-positive neuron, suggesting that each subtype shows a stereotyped pattern of migration during pupal development.

Intriguingly, many of Drf-positive neurons already projected to the lobula primordium in the larval brain (Fig. 6A,C). After projecting to the lobula, cell bodies began to migrate between 12 and 24 hours APF (Fig. 3A). At 24 hours APF, Drf-positive cell bodies were found in the inner area of the medulla cortex (Fig. 6D). Cell bodies were occasionally elongated with a radial orientation at 24 hours APF (arrowheads in Fig. 6D), which may imply these cells are migrating in radial orientation.

During pupal development, the medulla and lobula complex rotated 90° around the vertical axis, and the medulla cortex was eventually placed between the lamina and the medulla neuropile (Fig. 6D,E; Meinertzhagen and Hanson, 1993). The migration of medulla neurons may be a secondary effect of medulla rotation. However, the relative locations of the medulla cortex and the lamina at 24 hours APF were relatively unchanged when compared with the larval brain (Fig. 6C,D), suggesting that the medulla neurons independently migrate before the rotation that occurs after 24 hours APF.

Drf regulates axonal projections and dendritic arborizations

Because the *drf-Gal4* we used is not a strong loss-of-function allele, it is not suitable for an analysis of *drf* mutants. We thus searched for Gal4 drivers that could label Drf-positive neurons independently of *drf* gene expression. *NP2646* expressed *Gal4* in some types of medulla neurons, including Tm27(Y) neurons (Fig. S5). Tm27 neurons were rare, so we focused our analyses on Tm27Y. We created *drf* mutant MARCM clones and examined their morphology (Fig. 7). While wild-type Tm27Y neurons showed extensive arborizations at M4-5 and M8-10 in the medulla and targeted Lo4 in the lobula, loss of *drf* function caused reduced arborization at M8-10, ectopic arborization at M2-3 and axonal targeting defects in the lobula (Fig. 7,S5C-F). These defects are most likely caused by *drf* mutation because similar phenotypes were observed after using two independent *drf* alleles. Moreover, the defects were partially rescued by exogenous *drf* expression (Fig. S5C-F). The localization of Tm27Y cell bodies in the proximal to intermediate cortical zone was not noticeably altered in *drf* mutant clones (Fig. S5G). Essentially the same results were observed in Tm27 neurons (not shown). In other types of Drf-positive neurons, minor morphological defects were

observed by knocking down *drf* under the control of *drf-Gal4* (not shown).

Discussion

Neuronal identities are pre-determined in the larval medulla

Concentric genes are expressed in a defined subset of medulla neurons throughout development, suggesting that a part of neuronal identities are pre-determined in the larval medulla primordium. Our data suggest that Drf-positive neurons produce nine types of medulla neurons, including lobula projection and medulla intrinsic neurons, while Hth-positive neurons produce at least four types of neurons, including lamina projection and medulla intrinsic neurons. In Hth-positive neurons, Bsh is exclusively expressed in medulla intrinsic Mi1 neurons. A *hth* mutation caused the neuron to switch type (Fig. 5) while a *drf* mutation affected subsets of morphological features of Drf-positive neurons (Fig. 7). Thus, roles of concentric genes may be functionally segregated to form a genetic hierarchy. Apparently, other concentric genes must exist in addition to the four genes reported in this study. Because there are many neurons outside of the Drf domain in the larval medulla, some concentric genes may be

expressed in the outer zones. Some transcription factors may have expression patterns that differ from those of concentric genes, and their combined expression may specify restricted subtypes of medulla neurons. For example, *apterous* (*ap*) and Cut are widely expressed in medulla neurons (Fig. S4D; Morante and Desplan, 2008). Cut was co-expressed in subsets of Drf-positive neurons, while *ap* was expressed in all Drf- and Bsh/Hth-positive neurons (Fig. S4B and not shown).

Early born medulla neurons express the inner concentric genes while late born neurons express the outer ones. Thus, concentric gene expression correlates with neuronal birth order (Fig. 2). However, it is still unknown how concentric gene expression is specified. It would be possible to speculate that genes controlling temporal specification of neurons are expressed in NBs to control the concentric gene expression. However, the genes that are known to control neuronal birth order in the embryonic CNS were not expressed in larval medulla NBs (not shown; Isshiki et al. 2001). In addition to local, temporal mechanisms such as birth order, global and spatial mechanisms governed by morphogen gradient may also play a role in determining medulla cell type (Jessell, 2000). In addition to birth order or a morphogen gradient,

mutual repression among concentric genes may be essential in establishing defined concentric zones. Except for rare occasions, de-repression of other concentric genes was not induced in clones mutant for *hth* or *drf*. Additionally, ectopic *hth* expression did not compromise Drf and Run expression (not shown). These results may suggest that unidentified genes act redundantly with these genes to repress expression of other concentric genes and that weak Hth expression in NBs does not play roles in temporal specification of medulla neurons.

Regulation of migration and its biological significance

Various types of cell migration play important roles during vertebrate neurogenesis (Hatten, 1999; Nobrega-Pereira and Marin, 2009). Although *Drosophila* has been a powerful model of neural development, extensive neuronal migrations coupled with layer formation found in this study have not been previously reported. Our findings may establish a model to understand molecular mechanisms that govern brain development via neuronal migrations.

It is important to know whether the migration of medulla neurons occurs actively

or passively. The distribution of cell bodies in the adult medulla cortex was not random, but organized according to cell type (Fig. 3,S4). In particular, the Mi1 neurons identified by Bsh expression migrated outward and were eventually located in the outermost area of the adult medulla cortex (Fig. 3), which was affected in *hth* mutant clones (Fig. 5). The observation that defined localization of cell bodies is under the control of genetic program may not be explained by passive migration. Repression of apoptosis by expressing *p35* under the control of *elav-Gal4* did not compromise migration of Bsh- and Drf-positive neurons, suggesting that apoptosis is not a driving force of the migration (not shown). If neurons migrate actively in an organized manner, what regulates the pattern of migration? In many cases, glial cells play important roles in neuronal migration (Hatten, 1999). Indeed, we identified glial cells and their processes in the medulla cortex (Fig. 1G). Glial cells or other cell types could provide cues for neuronal migration.

The medulla neurons project axons near their targets forming subsets of dendrites in the larval brain (Fig. 5 and 6); the cell bodies migrated in the presence of preformed neurites during pupal development (Fig. 3). During or following cell body migration,

additional dendrites were formed along the axonal shafts (Fig. 5). Therefore, cell body migration may somehow contribute to circuit formation in the medulla. Indeed, similar strategies have been reported in sensory neurons of *C. elegans* and cerebellar granule cells in mammals (Heiman and Shaham, 2009; Solecki et al., 2006). Thus, cell body migration in the presence of neurites may be a general, conserved mechanism of circuit formation. Cell body migration may also allow developing cells to receive inductive cues provided by cells in the vicinity of the medulla cortex. For example, glial cells placed on the surface of the brain may trigger the expression of specific genes (e.g., *ChAT*) in Mi1 cells that are located in the outermost area of the adult medulla cortex.

Contributions to functional neuronal circuits

In adults, Mi1 neurons have arborization sites at M1 and M5, which coincide with the L1 lamina neuron terminals. In Golgi studies, Mi1 neurons were found in all parts of the retinotopic field (Fischbach and Dittrich, 1989). Indeed, the number of Bsh expressing medulla neurons was about 800, a figure similar to the number of ommatidial units (not shown). Therefore, the Mi1 neurons identified by Bsh expression are most likely

columnar neurons with direct inputs from L1 neurons. Because L1 is known to have inputs from R1-6, which processes motion detection, Mi1 may participate in the motion detection circuit (Fischbach and Dittrich, 1989; Joesch et al., 2010; Katsov and Clandinin, 2008; Rister et al., 2007; Zhu et al., 2009).

If the genetic codes that specify each type of neuron are found, it may encourage the functional study of defined neurons. In the medulla, *bsh-Gal4* is solely expressed by Mi1 neurons. Although the expression of Bsh is also observed in L4/5 lamina neurons (Zhu et al., 2009), intersectional strategies such as split Gal4 may enable us to specifically manipulate the activity of Mi1 by inducing expression of neurogenetic tools like *shibire*^{ts} (Kitamoto, 2001; Luan et al., 2006). Our findings may thus provide insight into high-resolution functional neurobiology in the *Drosophila* visual system.

Similarities with vertebrate neurogenesis

Development of the mammalian central nervous system reiteratively establishes cell identity, directs cell migration and assembles neuronal layers (Hatten, 1999), processes similar to the patterns observed during medulla development. In the cerebral cortex,

neurons are generated within the ventricular or subventricular zones and migrate outward, leaving their birthplace along the radial glial fibers. Later born neurons migrate radially into the cortical plate, past the deep layer neurons, and become the upper layers. The layers of the cortex are thus created inside-out (Nobrega-Pereira and Marin, 2009). In the developing spinal cord, neuronal types are specified according to morphogen gradients (Jessell, 2000). Within each domain along the dorso-ventral axis, neuronal and glial types are specified according to their birth order (Guillemot, 2007). The spinal cord neurons then migrate extensively along the radial, tangential and rostrocaudal axes (Leber and Sanes, 1995). Therefore, the initial organization of spinal cord neurons is disrupted in the mature system.

The medulla shares intriguing similarities with the mammalian central nervous system. For example, the concentric zones established in the larval medulla resemble the dorso-ventral subdivisions of the spinal cord (Jessell, 2000). Extensive migrations of medulla neurons disrupt concentric zones, as observed in the spinal cord. However, we found that the locations of cell bodies were organized according to neuronal type, a distribution that may be similar to the cortical organization of the cerebral cortex

(Nobrega-Pereira and Marin, 2009). Thus, the development of the medulla may share characteristics with various forms of neurogenesis found in the mammalian central nervous system. A comprehensive study of important features of neurogenesis will now be possible using the *Drosophila* visual center and powerful tools of *Drosophila* genetics. Unveiling all aspects of development in the medulla will not only shed light into the functional neurobiology of the visual system, but also elucidate the developmental neurobiology of vertebrates and invertebrates.

Acknowledgements

We thank Daiki Umetsu and Miyako Tai for the note that Bsh and Drf are expressed in concentric zones. We thank Karl Fischbach, Kei Ito, Tom Kornberg, Ian Meinertzhagen, Takaki Miyata, Koji Oishi, Michiya Sugimori, Shin-ya Takemura and Larry Zipursky for critical comments. We thank Haruhiro Higashida for use of facilities. We are grateful to Adi Salzberg, Masahide Asano, Ethan Bier, Sarah Certel, Takahiro Chihara, Shin-ichi Higashijima, Takako Isshiki, Kei Ito, Liqun Luo, Richard Mann, Chi-Hon Lee, William McGinnis, Andreas Prokop, James Skeath, Thomas Schwarz, Gary Struhl, Tadashi

Uemura, Larry Zipursky for antibodies, strains and plasmids. We thank BestGene for injection service, Bloomington Stock Center and DGRC, Kyoto for strains, DSHB and Asian Distribution Center for Segmentation Antibodies for antibodies and DGRC, Indiana for vectors. This work was supported by Program for Improvement of Research Environment for Young Researchers and PRESTO from JST, Takeda Science Foundation, Brain Science Foundation, Mitsubishi Foundation, Sumitomo Foundation, Uehara Memorial Foundation, Nakajima Foundation (to M.S.), Grants-in-Aid from MEXT (to M.S. and T.T.) and JSPS Research fellowship (to Y.K.).

Figure Legends

Figure 1. Larval medulla primordium is subdivided into concentric zones. (A-C) Schematics of the *Drosophila* visual system in third instar larva (A,B) and adult (C). Lateral (A) and horizontal views (B,C). (D-G) The larval medulla in lateral (D-G) and horizontal views (D'-G'). (D,D') Hth (green), Run (magenta) and Drf (blue) expression. (E,E') Hth (green) and Bsh (magenta) expression and NBs (Dpn; blue). Weak Hth expression in NE and NB cells (arrowhead in D' and arrows in D' and E', respectively). Bsh expression in lamina neurons (arrowhead in E'). (F,F') Hth (green) and Drf (blue) expression and neuronal projections (*elav-Gal4 UAS-CD8GFP*; white). Only GFP signal is shown in the right half (F). Primordia for medulla and lobula complex (arrows and arrowheads, respectively). (G,G') *hth-lacZ* (green), glial cell bodies (Repo; magenta) and glial processes (*repo-Gal4 UAS-CD8GFP*; white). Large and small glial cells in medulla cortex (arrows and arrowheads). Putative MNGs (large arrowheads). (H,I) Schematics of the concentric zones in larval medulla in lateral (H) and horizontal views (I). (J) Clones of larval medulla neurons expressing *CD8GFP* (green) and *tau-Myc* (magenta) under the control of *AyGal4*. Putative axons (arrows).

Figure 2. Birth order of medulla neurons correlates with concentric gene expression. (A,B) Clones of cells expressing *CD8GFP* (green). Drf (blue; arrowheads) and Bsh (magenta; arrowheads) expression and NBs (Dpn; magenta; arrows). Clones containing multiple NBs (A) or a single NB (B). (C) Number of cells expressing Drf, Bsh and Run in single NB clones that intersect the Drf-Bsh or Drf-Run domains. Clones in the posterior edge of the OPC are not considered. (D) A schematic of NBs producing multiple types of medulla neurons. (E,F) Neuronal birth order visualized by *dpn-Gal4 UAS-GFP* (green). Later born neurons show stronger GFP signals. (E) Drf (blue) and Bsh (magenta) expression. (F) Glial cells (Repo; magenta; arrowheads). (G,H) *Gal4* mRNA (magenta) expression in NBs (Dpn; blue) in *dpn-Gal4* flies. Lateral (G) and horizontal (H) views. (I) A schematic of the GFP gradient produced by NB specific Gal4 expression.

Figure 3. Medulla neurons migrate during pupal development. (A) Hth (green), Run (magenta) and Drf (blue) positive neurons in 8, 12, 16, 20, 24 hours APF pupal (A1-5)

and adult brains (A6). Run-positive cells in the outer zone (arrowhead in A2). Concentric zones are disrupted in 24 hours APF and adult brains (A5-6). (B) Hth (green) and Bsh (magenta) positive neurons and glial cells (Repo; blue) in 8, 12, 16, 20, 24 hours APF pupal (B1-5) and adult brains (B6). Hth/Bsh double positive neurons migrate outward (arrows). Putative MNGs (arrowheads). (C) Clones of medulla neurons visualized by *elav-Gal4 UAS-CD8GFP* (white; arrows) at late third instar (C1), 12 hours APF (C2) and 24 hours APF (C3) showing tangential migration between 12 and 24 hours APF. Lateral views.

Figure 4. Hth is expressed in four types of medulla neurons. (A) *hth-Gal4 UAS-nlsGFP* (green) overlaps Hth (red) in adult medulla. (B) *NP6013 UAS-CD8GFP* (white) overlaps Hth (green) in larval medulla. NCad (blue). Hth-positive neurons project to medulla but not to lobula complex (arrow and arrowhead). (C-F) Clones of Hth-positive neurons in adult medulla. NCad (blue) and *UAS>CD2>CD8GFP* (green) under the control of *hth-Gal4* (C,D,F) and *NP6013* (E). (C) Mi1, (D) Lawfl1, (E) Lawfl2 and (F) Pm3. (G) *bsh-Gal4 UAS-CD8GFP* (green) overlaps Bsh (red) in adult

medulla. NCad (blue). (H) Mi1: a clone expressing *UAS-CD8GFP* (green) and *UAS-SytHA* (red) under the control of *bsh-Gal4*. (I) Co-expression of ChAT (white) and Bsh (magenta) in adult medulla cortex.

Figure 5. *hth* regulates Bsh and NCad expression and neuronal identities. (A-C) Projections of *hth* mutant neurons labeled with *UAS-CD8GFP* (green) under the control of *hth-Gal4* (A,B; *hth-Gal4* clones) and *bsh-Gal4* (C; hth^{P2} clone) in adults. NCad (blue). Bsh (blue in A,B). (A) Irregular arborizations of Mi1-like neuron (arrowheads). (B,C) Tm13-like and Tm1-like neurons presumably transformed from Hth- and Bsh-positive neurons, respectively. Putative glial cells (arrowhead in B). (D) Catalogue of neurons in control, *hth* mutant and *hth* rescue clones. (E-I) Mi1 neurons of control (E-H) and $NCad^{M19}$ (I) clones at 0 (E,I), 20 (F), 24 hours APF (G) and adult (H) brains. Clones expressing *UAS-CD8GFP* (green) under the control of *NP6013* (E,I) or *bsh-Gal4* (F-H). NCad (magenta). Bsh (red in E,I). (E,F) Two arborization sites at 'Distal' and 'Proximal' NCad domains (arrowheads). (G) The arborizations of M1 are formed at 24 hours APF. 'Distal' and 'Proximal' arborizations in (E,F) correspond to

M5 and M9-10, respectively. (I) Proximal arborization is missing in *Ncad*^{M19} clones. (J) NCad up-regulation (white; arrow) in Hth domain (magenta) in larval medulla. Only NCad is shown in the right half. (K) Ectopic NCad up-regulation (white) in clones expressing *hth* (GFP; green; arrows). (L) Down-regulation of NCad (white) and Bsh expression (magenta) in *hth* mutant clones (dotted lines; arrows).

Figure 6. Drf is expressed in nine types of medulla neurons. (A) *drf-Gal4 UAS-CD8GFP* (white) overlaps Drf (red) in larval medulla. Medulla (arrows) and lobula complex (arrowheads). NCad (blue). (B) *drf-Gal4 UAS-nlsGFP* (white) overlaps Drf (red) in adult medulla. (C-E) *drf-Gal4 UAS-CD8GFP* (white), NCad (blue) and R-axons (Chaoptin; red) in larva (C), 24 hours APF pupa (D) and adult (E). Drf-neurons project to larval medulla and lobula complex (C). Distribution of Drf-neurons changes by 24 hours APF (D). Elongated cell bodies (arrowheads in D). Definition of layers in medulla (E3). Lateral (A) and horizontal views (B-E). (F-M) Nine types of Drf-positive neurons. Clones expressing *UAS-CD8GFP* (green) and *UAS-SytHA* (red) under the control of *drf-Gal4*. NCad (blue). (F) TmY3, (G) Tm27, (H) Tm27Y, (I) Tm9,

(J) Tm3a/b, (K) Mi10b, (L) Dm8a and (M) Dm8b. 3D reconstructed images (F1-M1) and single confocal sections (F2-M2,F3-J3,J4).

Figure 7. *drf* regulates axonal targeting and dendritic arborizations. Morphology of Tm27Y visualized by *NP2646 UAS-CD8GFP* (green) in control (A1-2) and drf^{E82} clones (B1-2) in adults. (A1,B1) Ectopic and reduced arborizations at M2-3 (arrows) and M8-10 (arrowheads) in medulla, respectively. (A2,B2) Axonal overshooting (arrows) and ectopic branch (arrowhead) in lobula. Lo4 defined by reduced NCad expression (blue; dotted lines).

References

Anderson, M. G., Perkins, G. L., Chittick, P., Shrigley, R. J. and Johnson, W. A. (1995). drifter, a Drosophila POU-domain transcription factor, is required for correct differentiation and migration of tracheal cells and midline glia. *Genes Dev* **9**, 123-37.

Bier, E., Vaessin, H., Younger-Shepherd, S., Jan, L. Y. and Jan, Y. N. (1992). deadpan, an essential pan-neural gene in Drosophila, encodes a helix-loop-helix protein similar to the hairy gene product. *Genes Dev* **6**, 2137-51.

Colonques, J., Ceron, J. and Tejedor, F. J. (2007). Segregation of postembryonic neuronal and glial lineages inferred from a mosaic analysis of the Drosophila larval brain. *Mech Dev* **124**, 327-40.

Egger, B., Boone, J. Q., Stevens, N. R., Brand, A. H. and Doe, C. Q. (2007). Regulation of spindle orientation and neural stem cell fate in the Drosophila optic lobe. *Neural Dev* **2**, 1.

Fischbach, K. F. and Dittrich, A. P. M. (1989). The optic lobe of Drosophila melanogaster. I. A Golgi analysis of wild-type structure. *Cell Tissue Res* **258**, 441-475.

Gao, S., Takemura, S. Y., Ting, C. Y., Huang, S., Lu, Z., Luan, H., Rister, J., Thum, A. S., Yang, M., Hong, S. T. et al. (2008). The neural substrate of spectral preference in Drosophila. *Neuron* **60**, 328-42.

Gergen, J. P. and Butler, B. A. (1988). Isolation of the Drosophila segmentation gene runt and analysis

of its expression during embryogenesis. *Genes Dev* **2**, 1179-93.

Gong, W. J. and Golic, K. G. (2003). Ends-out, or replacement, gene targeting in Drosophila. *Proc Natl Acad Sci U S A* **100**, 2556-61.

Guillemot, F. (2007). Spatial and temporal specification of neural fates by transcription factor codes. *Development* **134**, 3771-80.

Hatten, M. E. (1999). Central nervous system neuronal migration. *Annu Rev Neurosci* **22**, 511-39.

Heiman, M. G. and Shaham, S. (2009). DEX-1 and DYF-7 establish sensory dendrite length by anchoring dendritic tips during cell migration. *Cell* **137**, 344-55.

Hofbauer, A. and Campos-Ortega, J. A. (1990). Proliferation pattern and early differentiation of the optic lobes in Drosophila melanogaster. *Rouxs Arch. Dev. Biol.* **198**, 264-274.

Isshiki, T., Pearson, B., Holbrook, S. and Doe, C. Q. (2001). Drosophila neuroblasts sequentially express transcription factors which specify the temporal identity of their neuronal progeny. *Cell* **106**, 511-21.

Ito, K., Awano, W., Suzuki, K., Hiromi, Y. and Yamamoto, D. (1997). The Drosophila mushroom body is a quadruple structure of clonal units each of which contains a virtually identical set of neurones and glial cells. *Development* **124**, 761-71.

Iwai, Y., Usui, T., Hirano, S., Steward, R., Takeichi, M. and Uemura, T. (1997). Axon patterning requires DN-cadherin, a novel neuronal adhesion receptor, in the Drosophila embryonic CNS. *Neuron* **19**, 77-89.

Jessell, T. M. (2000). Neuronal specification in the spinal cord: inductive signals and transcriptional codes. *Nat Rev Genet* **1**, 20-9.

Joesch, M., Schnell, B., Raghu, S. V., Reiff, D. F. and Borst, A. (2010). ON and OFF pathways in *Drosophila* motion vision. *Nature* **468**, 300-304.

Jones, B. and McGinnis, W. (1993). A new Drosophila homeobox gene, bsh, is expressed in a subset of brain cells during embryogenesis. *Development* **117**, 793-806.

Kaphingst, K. and Kunes, S. (1994). Pattern formation in the visual centers of the Drosophila brain: wingless acts via decapentaplegic to specify the dorsoventral axis. *Cell* **78**, 437-48.

Katsov, A. Y. and Clandinin, T. R. (2008). Motion processing streams in Drosophila are behaviorally specialized. *Neuron* **59**, 322-35.

Kimura, Y., Okamura, Y. and Higashijima, S. (2006). alx, a zebrafish homolog of Chx10, marks ipsilateral descending excitatory interneurons that participate in the regulation of spinal locomotor circuits. *J Neurosci* **26**, 5684-97.

Kitamoto, T. (2001). Conditional modification of behavior in Drosophila by targeted expression of a temperature-sensitive shibire allele in defined neurons. *J Neurobiol* **47**, 81-92.

Kosman, D., Small, S. and Reinitz, J. (1998). Rapid preparation of a panel of polyclonal antibodies to Drosophila segmentation proteins. *Dev Genes Evol* **208**, 290-4.

Kurant, E., Pai, C. Y., Sharf, R., Halachmi, N., Sun, Y. H. and Salzberg, A. (1998). Dorsotonals/homothorax, the Drosophila homologue of meis1, interacts with extradenticle in patterning of the embryonic PNS. *Development* **125**, 1037-48.

Leber, S. M. and Sanes, J. R. (1995). Migratory paths of neurons and glia in the embryonic chick spinal cord. *J Neurosci* **15**, 1236-48.

Lee, C. H., Herman, T., Clandinin, T. R., Lee, R. and Zipursky, S. L. (2001). N-cadherin regulates target specificity in the Drosophila visual system. *Neuron* **30**, 437-50.

Lee, T. and Luo, L. (1999). Mosaic analysis with a repressible cell marker for studies of gene function in neuronal morphogenesis. *Neuron* **22**, 451-61.

Llimargas, M. and Casanova, J. (1997). ventral veinless, a POU domain transcription factor, regulates different transduction pathways required for tracheal branching in Drosophila. *Development* **124**, 3273-81.

Luan, H., Peabody, N. C., Vinson, C. R. and White, B. H. (2006). Refined spatial manipulation of neuronal function by combinatorial restriction of transgene expression. *Neuron* **52**, 425-36.

McGuire, S. E., Le, P. T., Osborn, A. J., Matsumoto, K. and Davis, R. L. (2003). Spatiotemporal rescue of memory dysfunction in Drosophila. *Science* **302**, 1765-8.

Meinertzhagen, I. A. and Hanson, T. E. (1993). The development of the optic lobe. In *The development of Drosophila melanogaster*, (ed. M. Bate and A. Martinez-Arias), pp. 1363-1491. Cold Spring Harbor Laboratory, NY: Cold Spring Harbor Laboratory Press.

Morante, J. and Desplan, C. (2008). The color-vision circuit in the medulla of Drosophila. *Curr Biol* **18**, 553-65.

Nassif, C., Noveen, A. and Hartenstein, V. (2003). Early development of the Drosophila brain: III. The pattern of neuropile founder tracts during the larval period. *J Comp Neurol* **455**, 417-34.

Nern, A., Zhu, Y. and Zipursky, S. L. (2008). Local N-cadherin interactions mediate distinct steps in the targeting of lamina neurons. *Neuron* **58**, 34-41.

Nobrega-Pereira, S. and Marin, O. (2009). Transcriptional control of neuronal migration in the developing mouse brain. *Cereb Cortex* **19 Suppl 1**, i107-13.

Pai, C. Y., Kuo, T. S., Jaw, T. J., Kurant, E., Chen, C. T., Bessarab, D. A., Salzberg, A. and Sun, Y. H.

(1998). The Homothorax homeoprotein activates the nuclear localization of another homeoprotein, extradenticle, and suppresses eye development in Drosophila. *Genes Dev* **12**, 435-46.

Rieckhof, G. E., Casares, F., Ryoo, H. D., Abu-Shaar, M. and Mann, R. S. (1997). Nuclear translocation of extradenticle requires homothorax, which encodes an extradenticle-related homeodomain protein. *Cell* **91**, 171-83.

Rister, J., Pauls, D., Schnell, B., Ting, C. Y., Lee, C. H., Sinakevitch, I., Morante, J., Strausfeld, N. J., Ito, K. and Heisenberg, M. (2007). Dissection of the Peripheral Motion Channel in the Visual System of Drosophila melanogaster. *Neuron* **56**, 155-70.

Robinson, I. M., Ranjan, R. and Schwarz, T. L. (2002). Synaptotagmins I and IV promote transmitter release independently of Ca(2+) binding in the C(2)A domain. *Nature* **418**, 336-40.

Sanes, J. R. and Zipursky, S. L. (2010). Design principles of insect and vertebrate visual systems. *Neuron* **66**, 15-36.

Sato, M., Umetsu, D., Murakami, S., Yasugi, T. and Tabata, T. (2006). DWnt4 regulates the dorsoventral specificity of retinal projections in the Drosophila melanogaster visual system. *Nat Neurosci* **9**, 67-75.

Sepp, K. J. and Auld, V. J. (1999). Conversion of lacZ enhancer trap lines to GAL4 lines using targeted

transposition in Drosophila melanogaster. *Genetics* **151**, 1093-101.

Solecki, D. J., Govek, E. E., Tomoda, T. and Hatten, M. E. (2006). Neuronal polarity in CNS development. *Genes Dev* **20**, 2639-47.

Struhl, G. and Basler, K. (1993). Organizing activity of wingless protein in Drosophila. *Cell* **72**, 527-40.

Takemura, S. Y., Lu, Z. and Meinertzhagen, I. A. (2008). Synaptic circuits of the Drosophila optic lobe: the input terminals to the medulla. *J Comp Neurol* **509**, 493-513.

Thor, S., Andersson, S. G., Tomlinson, A. and Thomas, J. B. (1999). A LIM-homeodomain combinatorial code for motor-neuron pathway selection. *Nature* **397**, 76-80.

Ting, C. Y., Yonekura, S., Chung, P., Hsu, S. N., Robertson, H. M., Chiba, A. and Lee, C. H. (2005). Drosophila N-cadherin functions in the first stage of the two-stage layer-selection process of R7 photoreceptor afferents. *Development* **132**, 953-63.

Tix, S., Eule, E., Fischbach, K. F. and Benzer, S. (1997). Glia in the chiasms and medulla of the Drosophila melanogaster optic lobes. *Cell Tissue Res* **289**, 397-409.

Toriya, M., Tokunaga, A., Sawamoto, K., Nakao, K. and Okano, H. (2006). Distinct functions of human numb isoforms revealed by misexpression in the neural stem cell lineage in the Drosophila larval brain. *Dev Neurosci* **28**, 142-55.

Venken, K. J., He, Y., Hoskins, R. A. and Bellen, H. J. (2006). P[acman]: a BAC transgenic platform for targeted insertion of large DNA fragments in D. melanogaster. *Science* **314**, 1747-51.

Wong, A. M., Wang, J. W. and Axel, R. (2002). Spatial representation of the glomerular map in the Drosophila protocerebrum. *Cell* **109**, 229-41.

Yasugi, T., Umetsu, D., Murakami, S., Sato, M. and Tabata, T. (2008). Drosophila optic lobe neuroblasts triggered by a wave of proneural gene expression that is negatively regulated by JAK/STAT. *Development* **135**, 1471-80.

Zhu, Y., Nern, A., Zipursky, S. L. and Frye, M. A. (2009). Peripheral visual circuits functionally segregate motion and phototaxis behaviors in the fly. *Curr Biol* **19**, 613-9.

Fig1

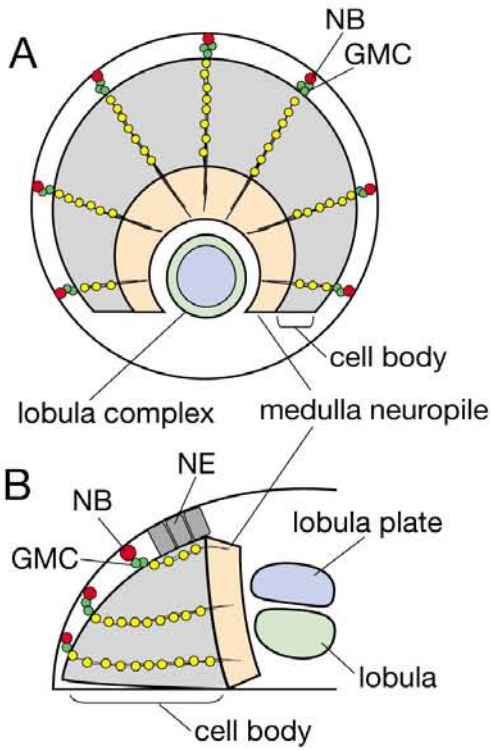
A
NB
GMC
cell body
lobula complex
medulla neuropile
B
NE
NB
GMC
lobula plate
lobula
cell body

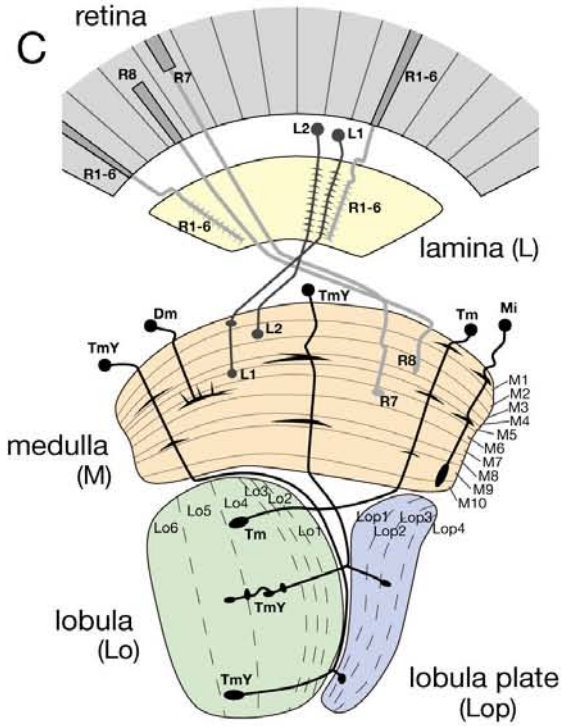
C
retina
R8
R7
R1-6
L2
L1
lamina (L)
Dm
TmY
Tm
Mi
medulla
(M)
M1
M2
M3
M4
M5
M6
M7
M8
M9
M10
Lo1
Lo2
Lo3
Lo4
Lo5
Lo6
Lop1
Lop2
Lop3
Lop4
lobula
(Lo)
lobula plate
(Lop)

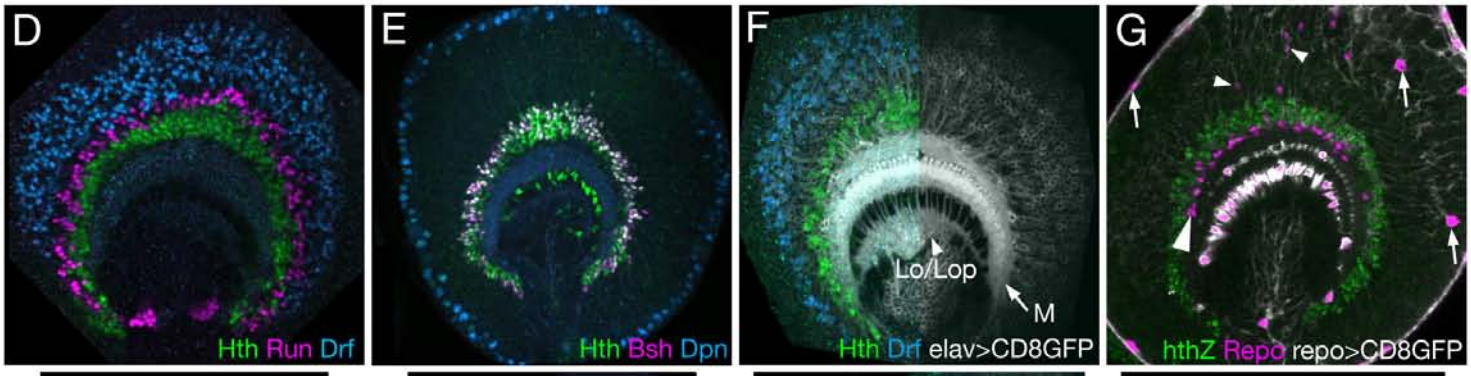
D
Hth Run Drf
E
Hth Bsh Dpn
F
Lo/Lop
M
Hth Drf elav>CD8GFP
G
hthZ Repo repo>CD8GFP
lateral

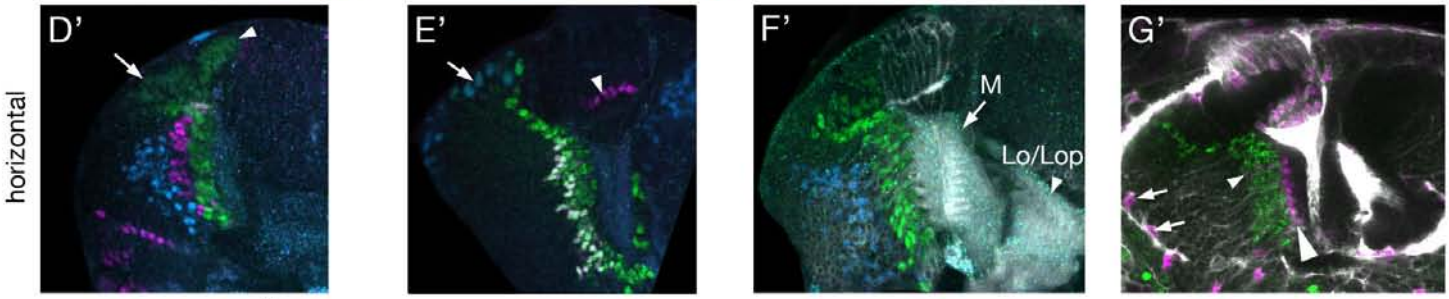
D'
E'
F'
M
Lo/Lop
G'
horizontal

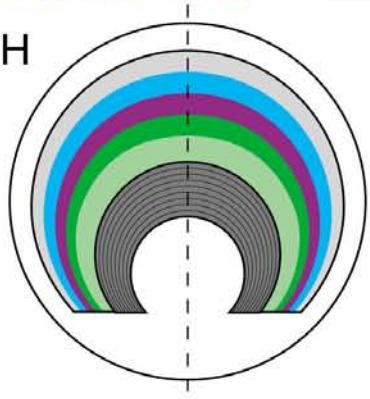
H

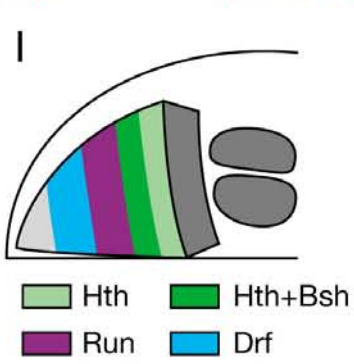
I
Hth
Hth+Bsh
Run
Drf

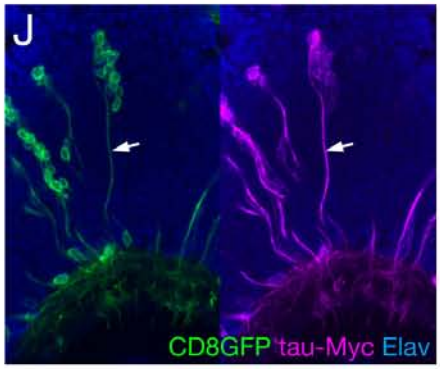
J
CD8GFP tau-Myc Elav

Fig2

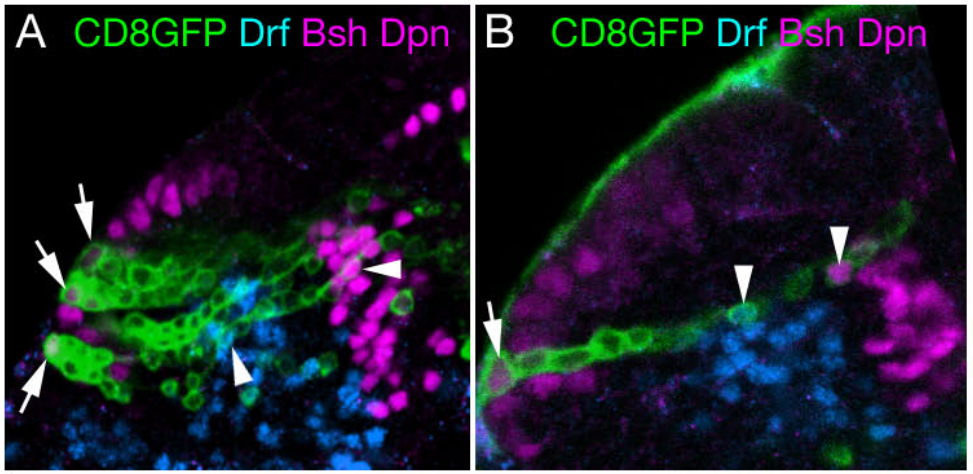

C

Drf+	Bsh+	clones
3	1	6
2	1	7
		n=13

Drf+	Run+	clones
4	1	2
3	1	4
2	1	10
1	1	2
		n=18

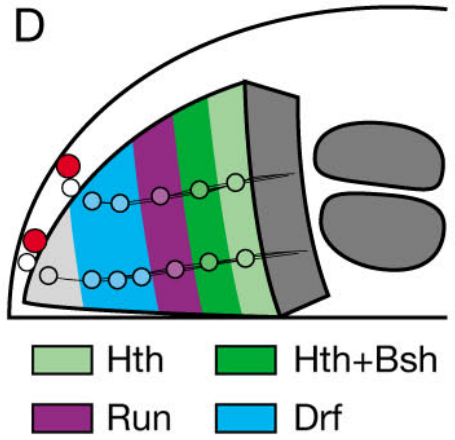

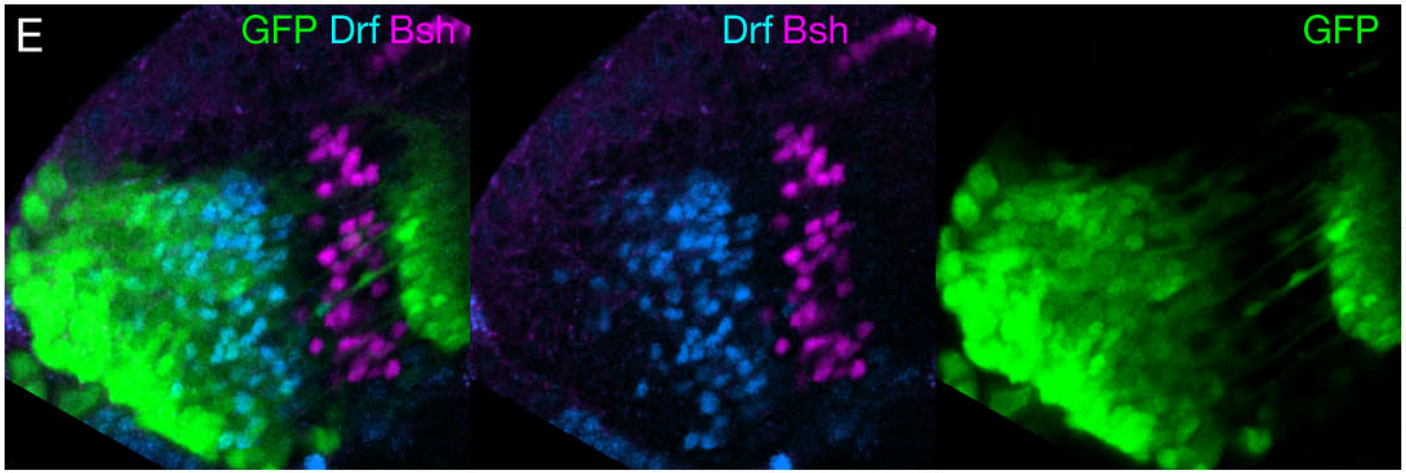

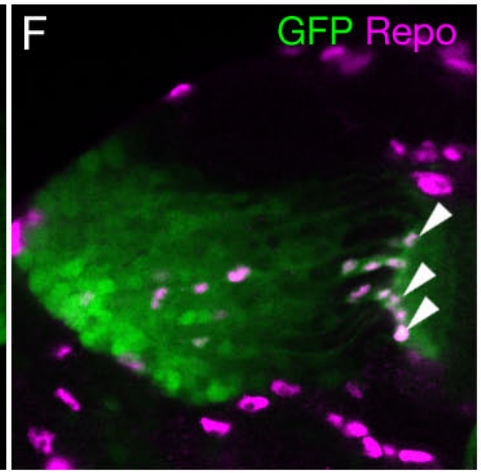

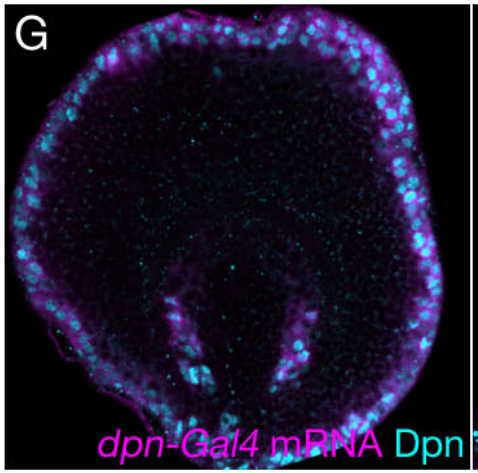

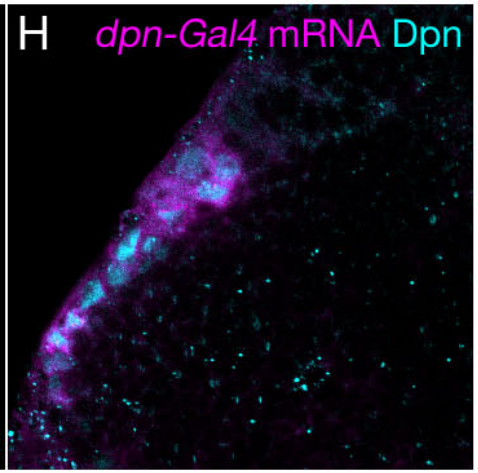

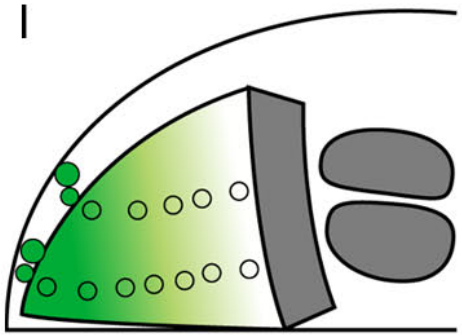

Fig3

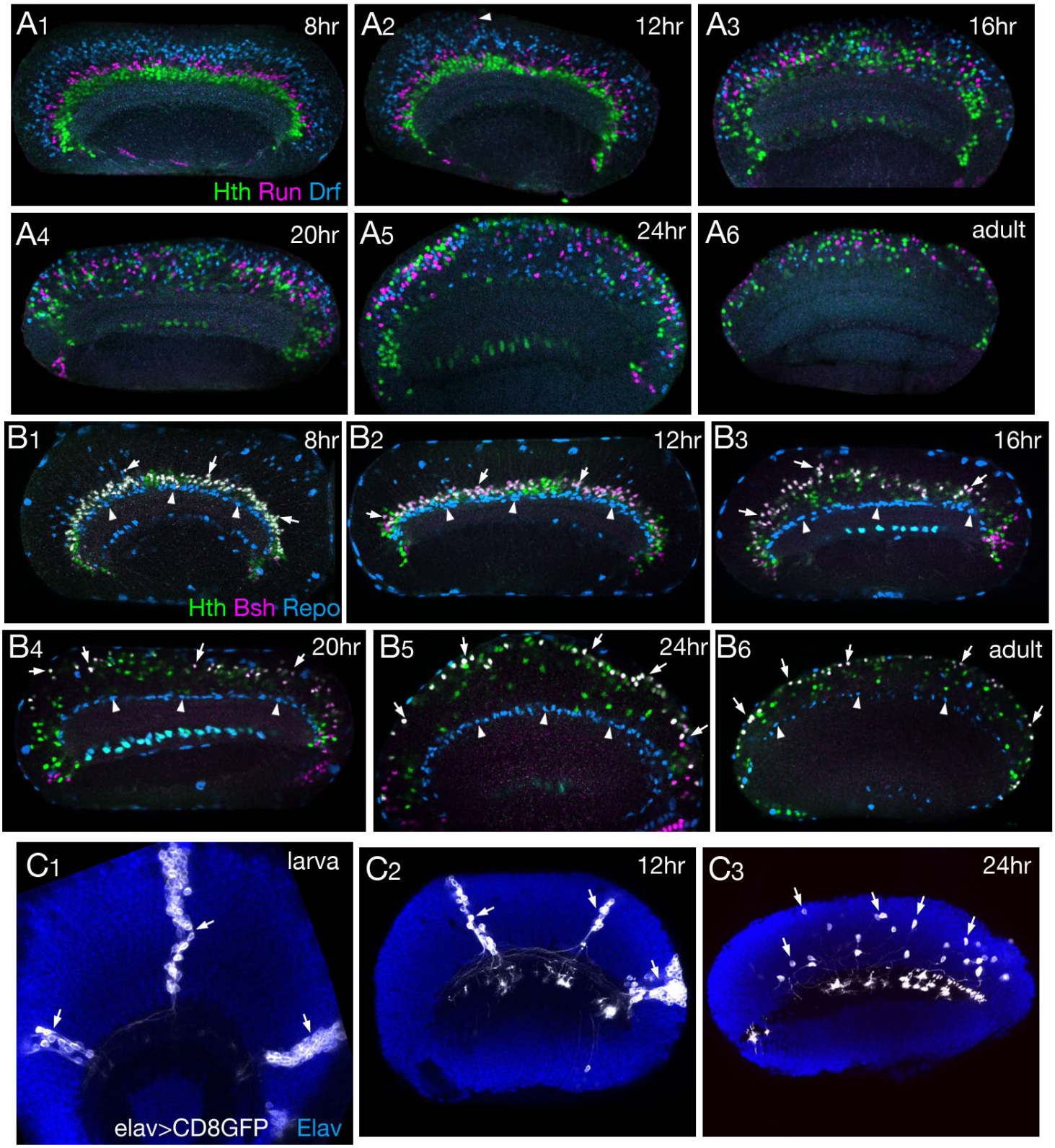
A1
8hr
Hth Run Drf
A2
12hr
A3
16hr
A4
20hr
A5
24hr
A6
adult
B1
8hr
Hth Bsh Repo
B2
12hr
B3
16hr
B4
20hr
B5
24hr
B6
adult
C1
larva
elav>CD8GFP Elav
C2
12hr
C3
24hr

Fig4

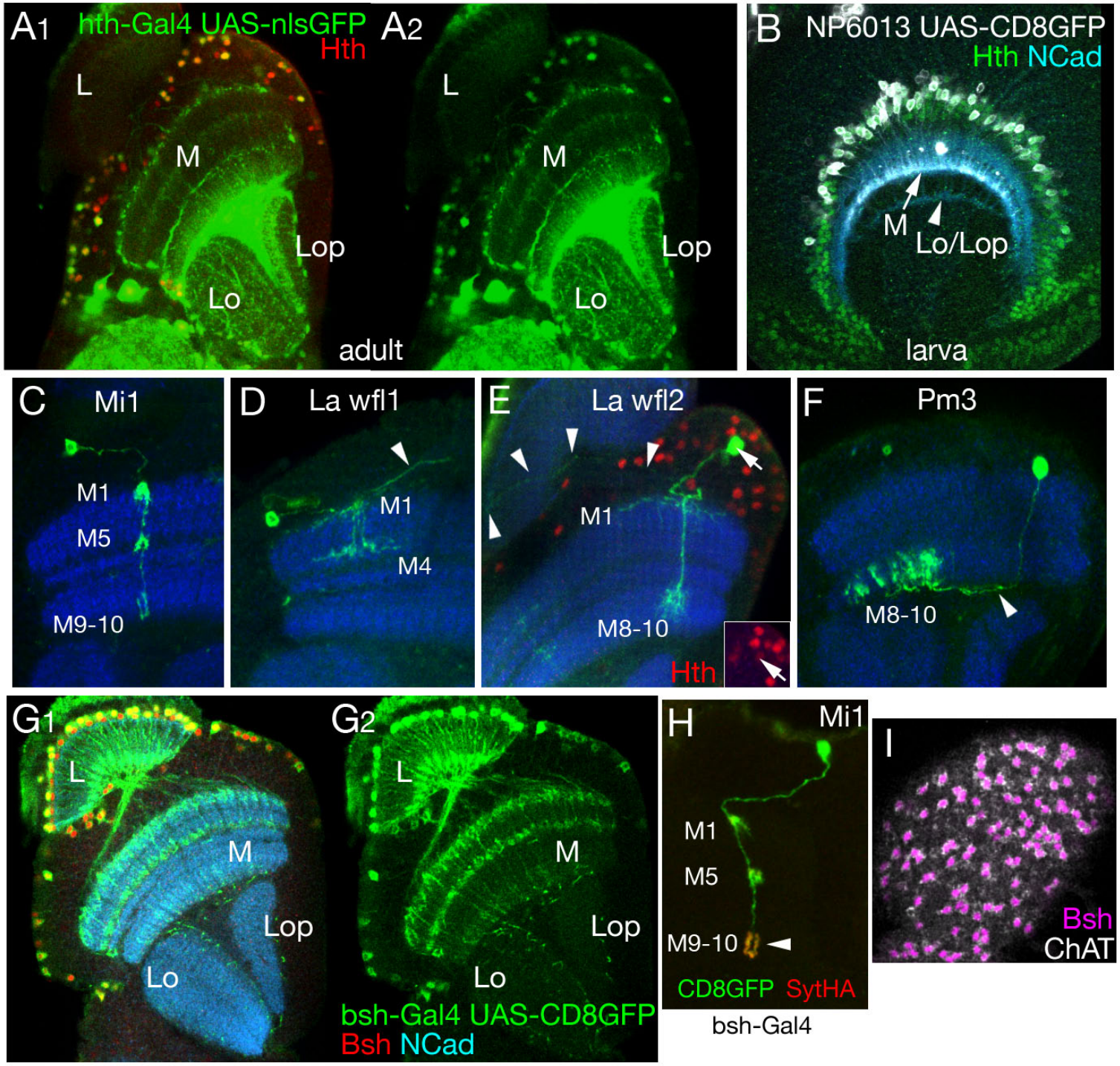
A1
hth-Gal4 UAS-nlsGFP
Hth
L
M
Lop
Lo
adult
A2
L
M
Lop
Lo
B
NP6013 UAS-CD8GFP
Hth NCad
M
Lo/Lop
larva
C
Mi1
M1
M5
M9-10
D
La wfl1
M1
M4
E
La wfl2
M1
M8-10
Hth
F
Pm3
M8-10
G1
L
M
Lop
Lo
G2
L
M
Lop
Lo
bsh-Gal4 UAS-CD8GFP
Bsh NCad
H
Mi1
M1
M5
M9-10
CD8GFP SytHA
bsh-Gal4
I
Bsh
ChAT

Fig 5

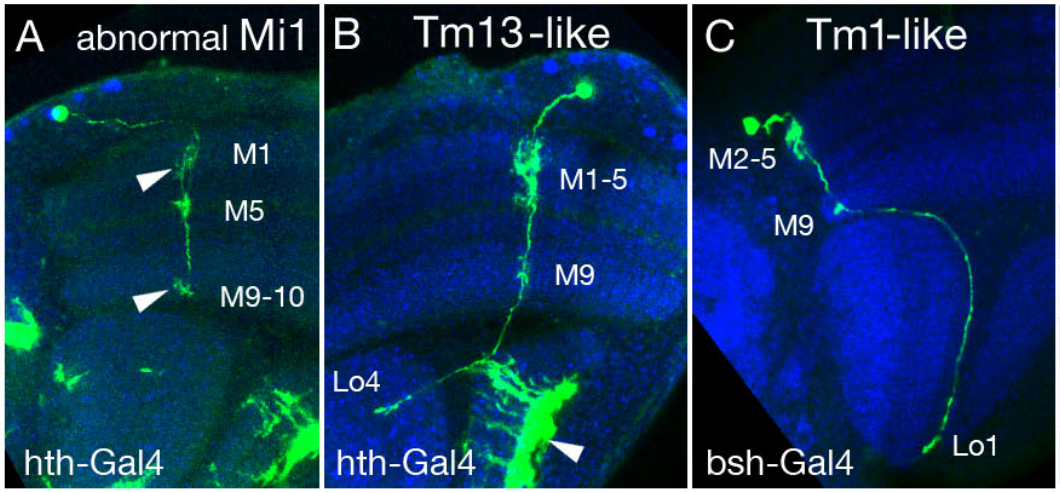

D	hth-Gal4 ctrl	hth-Gal4 mutant	hth-Gal4 mutant rescue	bsh-Gal4 ctrl	bsh-Gal4 hth^{P2}	bsh-Gal4 hth^{P2} rescue
Mi1	115	0	33	138	15	34
abnormal Mi1	0	3	3	0	8	0
La wfl1	15	0	0	0	0	0
La wfl2	0	1	0	0	0	0
Pm3	2	0	0	0	0	0
Hth negative	0	75	9	0	65	47
total	132	79	45	138	88	81

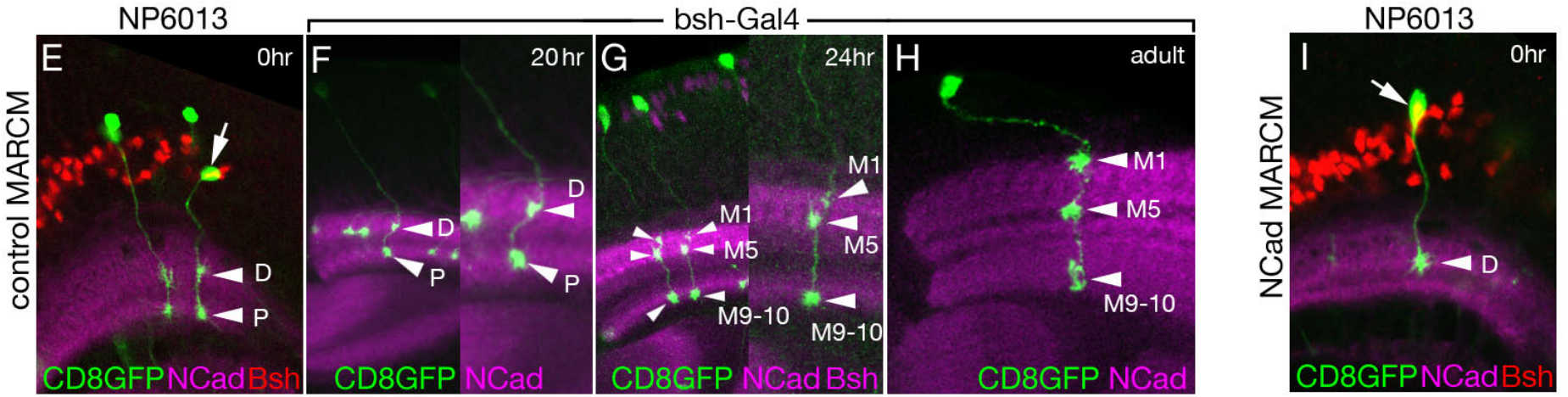

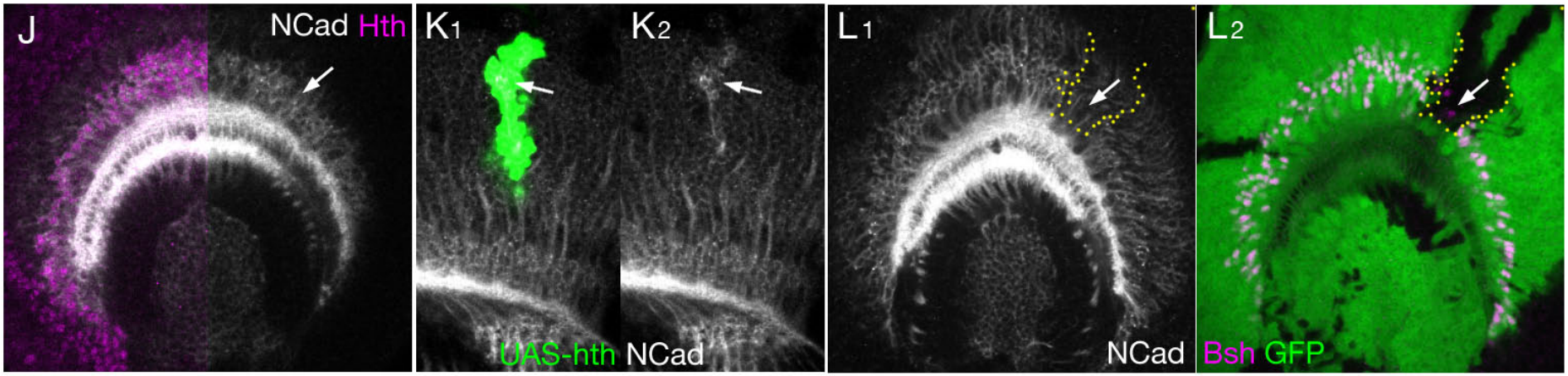

Fig 6

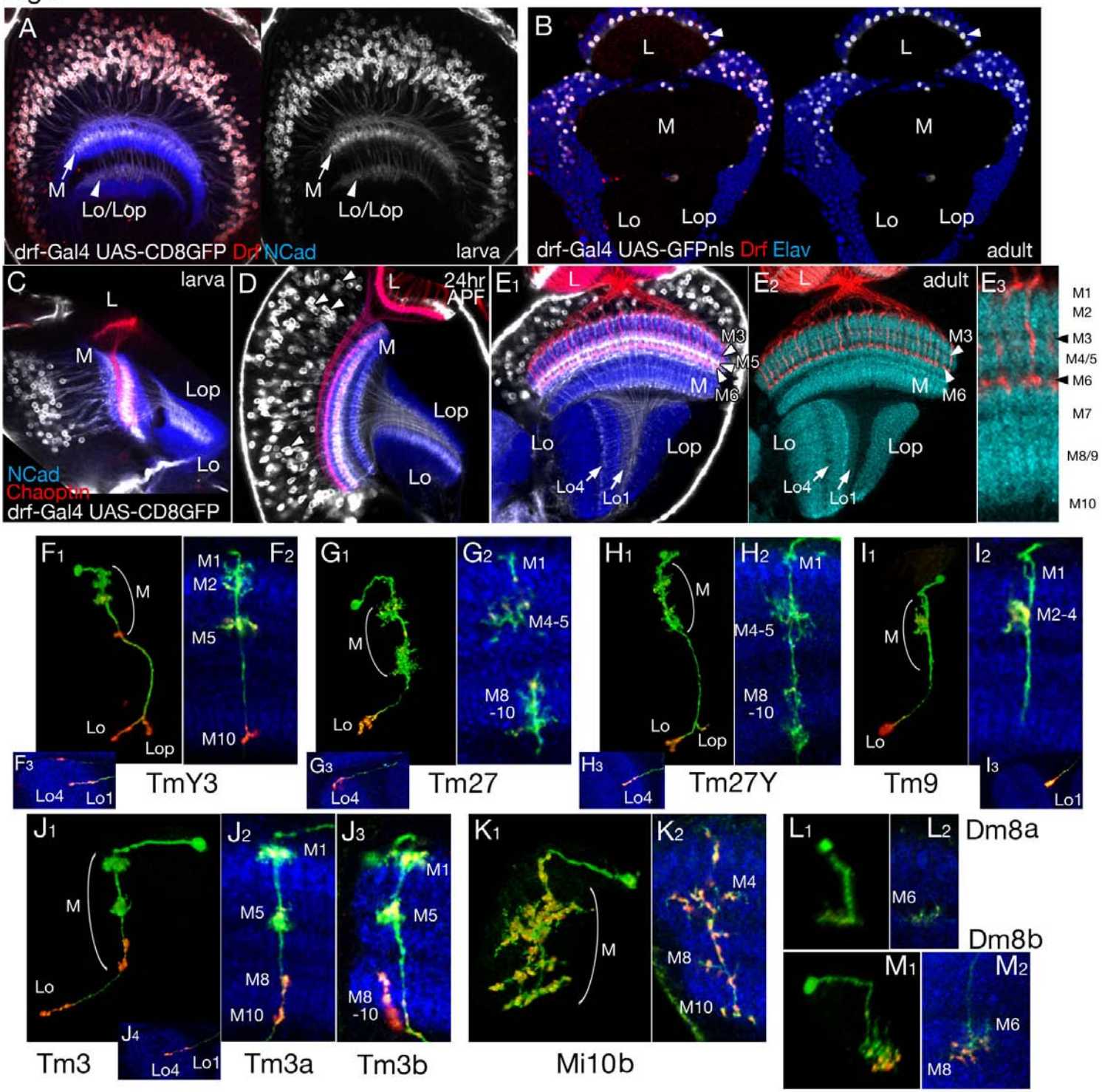
A
M
Lo/Lop
drf-Gal4 UAS-CD8GFP Drf NCad
larva
B
L
M
Lo
Lop
drf-Gal4 UAS-GFPnls Drf Elav
adult
C
larva
L
M
Lop
Lo
NCad
Chaoptin
drf-Gal4 UAS-CD8GFP
D
L
24hr APF
M
Lop
Lo
E1
L
M3
M5
M
M6
Lo
Lop
Lo4
Lo1
E2
adult
E3
M1
M2
M3
M4/5
M6
M7
M8/9
M10
F1
F2
M1
M2
M5
M10
Lo
Lop
F3
Lo4
Lo1
TmY3
G1
G2
M4-5
M8
-10
G3
Tm27
H1
H2
Tm27Y
I1
I2
M2-4
I3
Tm9
J1
J2
J3
J4
Tm3
Tm3a
Tm3b
K1
K2
Mi10b
L1
L2
M6
Dm8a
Dm8b
M1
M2
M8

Fig 7

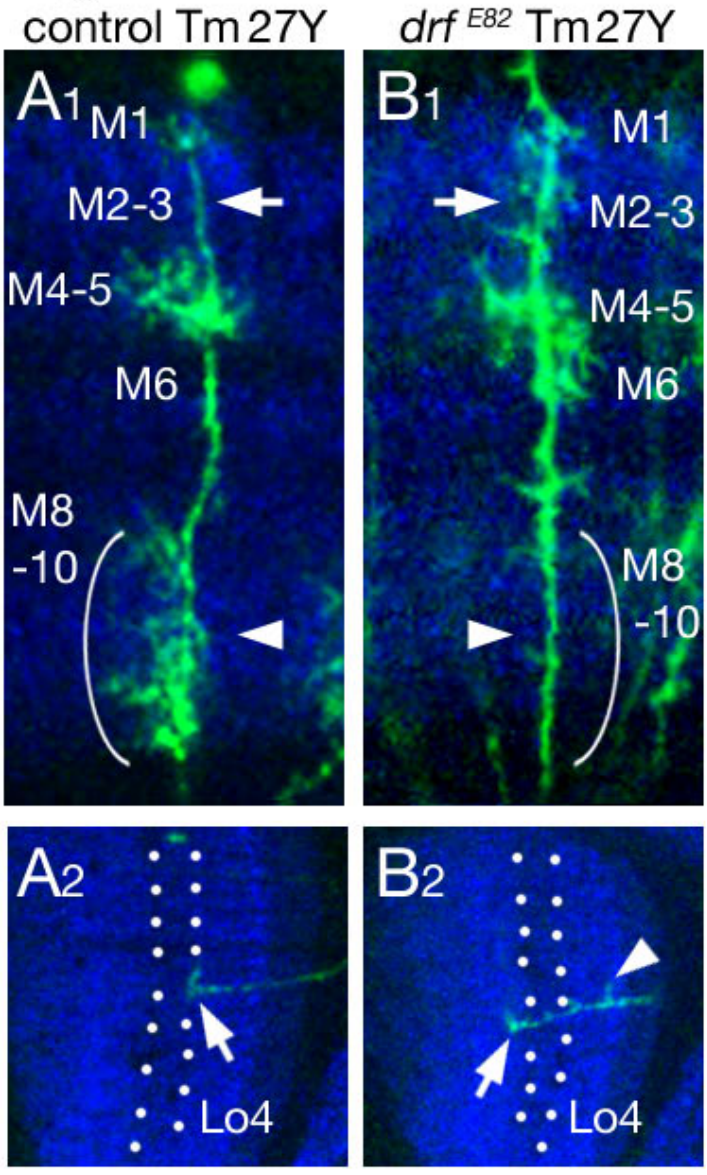
control Tm27Y
drf E82 Tm27Y
A1
M1
M2-3
M4-5
M6
M8
-10
B1
M1
M2-3
M4-5
M6
M8
-10
A2
Lo4
B2
Lo4

Supplementary Materials

Figure S1

A.

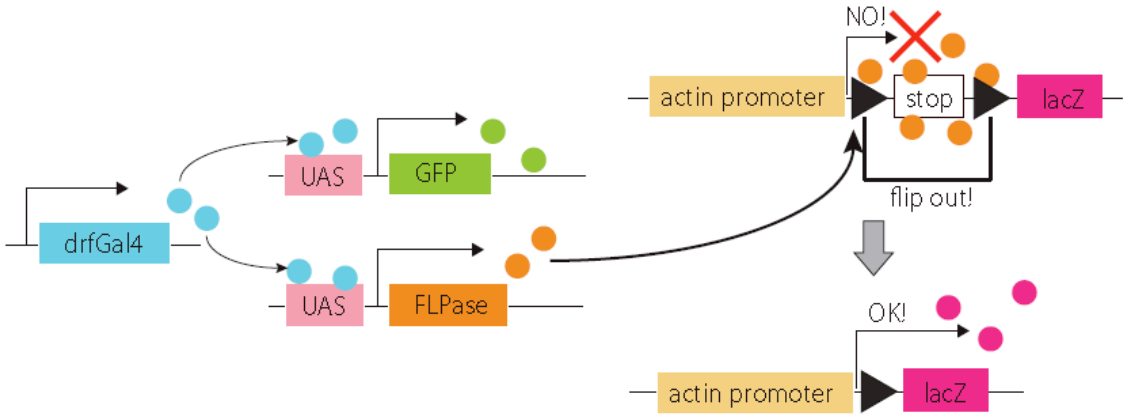

B.

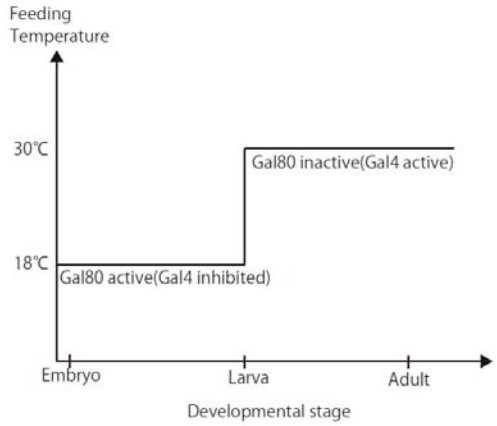

C.

Fly	lacZ positive	lacZ,GFP positive
1	63	63
2	52	52
3	55	55
4	51	51
5	66	66
Total	287	287

D.

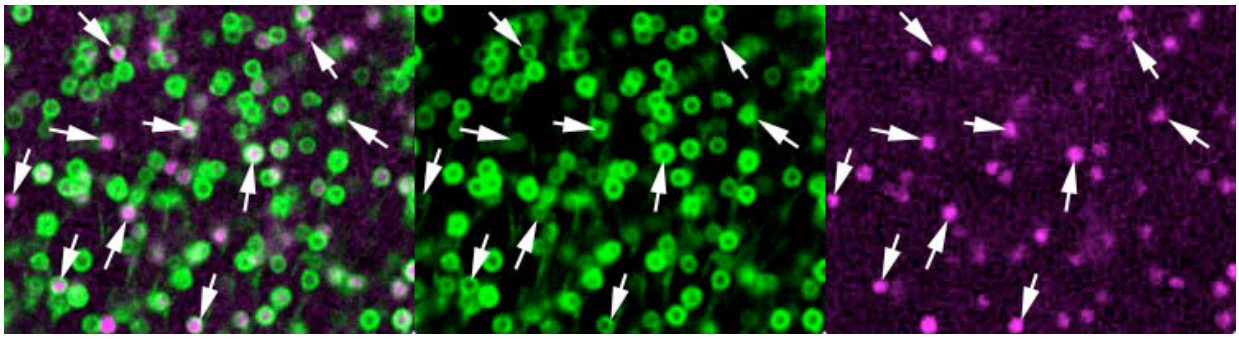

UAS-flp; Gal80^{ts}; drf-Gal4 UAS-CD8GFP / act>stop>lacZ GFP LacZ

Figure S1. *drf* expression persists in Drf-positive medulla neurons during metamorphosis.

(A) Gal4 protein produced in *drf* expressing cells activates expression of GFP and FLPase, which

then induces somatic recombination between two FRT sites releasing lacZ expression in the flip-out lacZ construct. Subsets of Drf-positive neurons are constitutively labeled with LacZ. (B) In the presence of *tubulin-Gal80^{TS}*, Gal4-induced FLPase expression is repressed at 18°C prior to third larval instar, but is then activated at 30°C during pupal development. (C) In five independent adult brains, number of LacZ positive cells were identical to that of LacZ/GFP double positive cells, suggesting that *drf* expression as revealed by GFP signal persists in the LacZ expressing cells. (D) Expression of LacZ (magenta) and GFP (green) is compared in the adult medulla cortex. While LacZ-positive cells are always GFP-positive, LacZ is not always expressed in GFP-positive cells. FLPase induced recombination between the FRT sites may be inefficient in the medulla due to an unknown reason.

Figure S2

A.

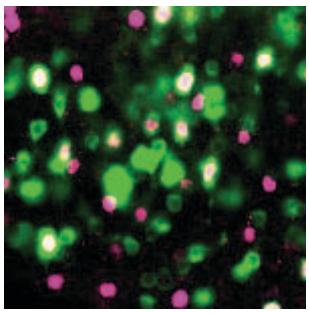

B.

	hth-Gal4	NP6013	Bsh	Hth
Mi1	94	7	+	+
La wfl1	5	0	-	+
La wfl2	0	11	-	+
Pm3	2	0	-	+
total	101	18		

Figure S2. A catalogue of Hth- and Bsh-positive neurons.

(A) *NP6013 UAS-CD8GFP* expression (green) is found in a subset of Hth-positive neurons (magenta) in the adult medulla cortex. (B) A catalogue of Hth-positive medulla neurons labeled with *UAS>CD2>CD8GFP* under the control of *hth-Gal4* and *NP6013*. Hth is expressed in Mi1, La wfl1, La wfl2 and Pm3, while Bsh is solely expressed in Mi1.

Figure S3

A.

	hth-Gal4 ctrl	hth-Gal4 mutant	hth-Gal UAS-hth	bsh-Gal4 ctrl	bshGal4 hth^{P2}	bsh-Gal4 hth^{P2} UAS-hth
Mi1	115	0	33	138	15	34
abnormal Mi1	0	3	3	0	8	0
La wfl1	15	0	0	0	0	0
La wfl2	0	1	0	0	0	0
Pm3	2	0	0	0	0	0
Mi(1-3) lamina	0	5	0	0	0	0
Other Mi	0	1	0	0	0	0
Tm1(a)-like	0	2	0	0	57	35
Tm2-like	0	1	0	0	0	0
Tm3-like	0	24	4	0	0	2
Tm4-like	0	4	0	0	0	0
Tm5-like	0	1	0	0	2	1
Tm6-like	0	0	1	0	0	0
Tm9-like	0	3	1	0	0	0
Tm11-like	0	1	0	0	0	0
Tm12-like	0	4	0	0	0	0
Tm13-like	0	8	1	0	0	0
Tm14-like	0	1	0	0	0	1
Tm20-like	0	4	0	0	0	0
Other Tm	0	10	2	0	5	5
TmY3-like	0	2	0	0	0	0
Other TmY	0	1	0	0	1	2
Others	0	3	0	0	0	1
Total	132	79	45	138	88	81

B. hth^{P2} MARCM clone Elav Pros GFP

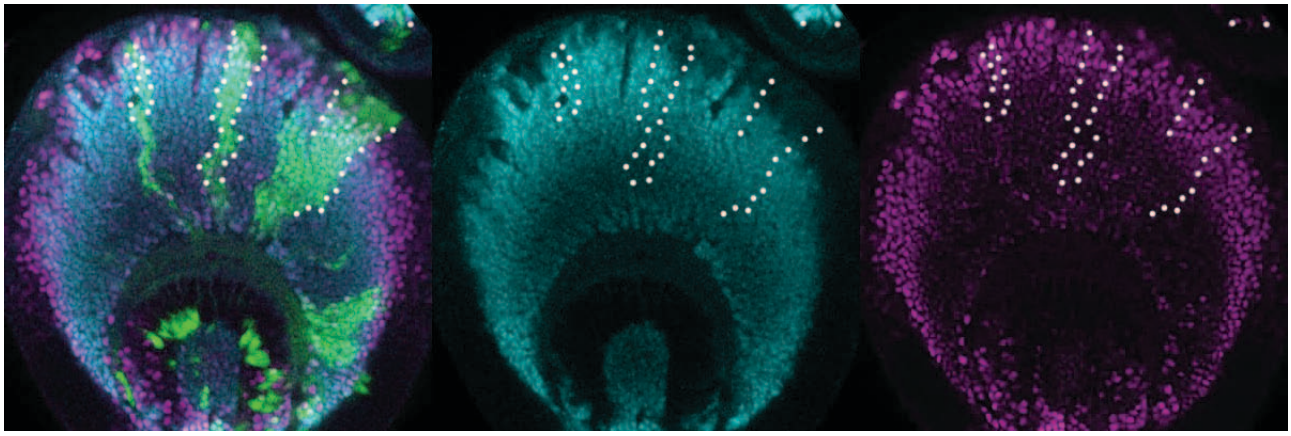

Figure S3. Transformation of neuronal types in *hth* mutant clones.

(A) A catalogue of medulla neurons labeled with *hth-Gal4* and *bsh-Gal4* in various genetic backgrounds. In *hth-Gal4* homozygous clones, Mi1-like abnormal neurons were occasionally found instead of Mi1. Additionally, Tm type lobula projection neurons were frequently observed. While *bsh-Gal4* solely labels Mi1 in the control background, Mi1-like abnormal neurons and Tm1-like neurons were observed in *hth^{P2}* homozygous clones. Tm3-like and Tm1-like neurons were frequently observed in *hth-Gal4* homozygous clones and *hth^{P2}* clones with *bsh-Gal4*, respectively. The variation of phenotypes in the two experiments may be caused by difference in the *hth* alleles and/or Gal4 drivers. The defects were partially rescued by introducing *UAS-hth*. Inefficient rescue by *bsh-Gal4 UAS-hth* may be due to weak Gal4 expression during larval development. (B) *hth^{P2}* homozygous clones labeled with GFP (green; dotted lines), Prospero (magenta) and Elav (blue) in the larval medulla primordium. Production of GMCs and neurons is not affected.

Figure S4

A.

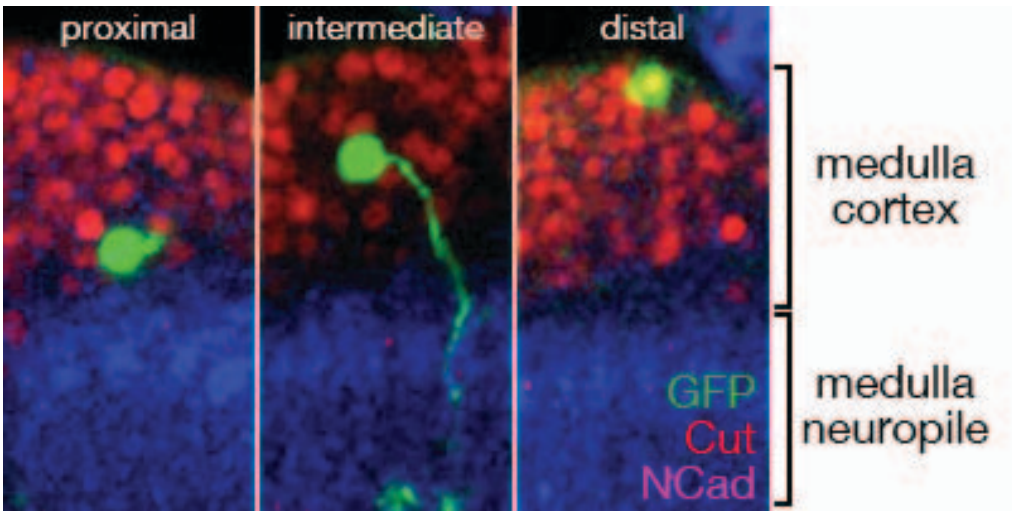

B.

Neuronal type	Proximal	Intermediate	Distal	n	Cut	Dac	Drf
Mi10b	0	2	7	9	++	-	+++
Tm3a	0	1	19	20	++	-	+++
Tm3b	0	0	9	10	++	-	+++
Dm8a	0	2	7	9	-	+	+
Tm9	2	16	2	20	+	+	++
Dm8b	0	8	3	11	-	+	+
TmY3	1	17	6	24	-	-	+++
Tm27Y	8	16	1	25	-	-	+++
Tm27	7	4	0	11	-	-	+++

C. Dac Drf□□□□□□□□□□□□□□□D. Cut Drf

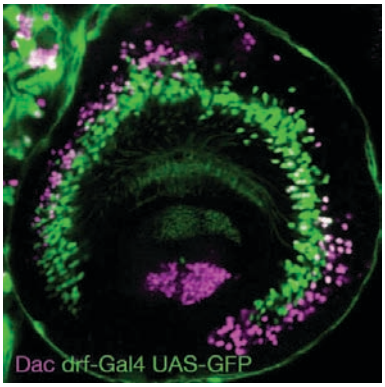

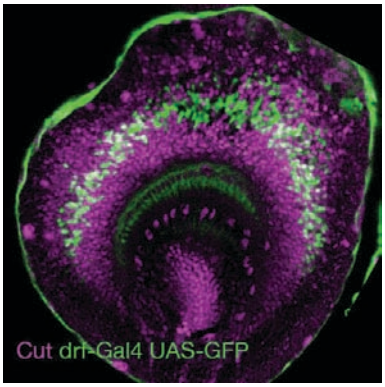

Figure S4. Location of cell body correlates with neuronal subtypes of Drf-positive neurons.
(A) Locations of cell bodies in the medulla cortex were categorized into equally divided three zones: distal, intermediate and proximal. NCad (magenta), GFP (green) and Cut (red). (B) Locations of cell bodies for each subtype of Drf-positive neurons were examined. The expression profiles of Cut, Dac and Drf shown in the right table reveal that each subtype shows a specific combination of Cut, Dac and Drf expression. These three factors and unidentified factors may be involved in specifying neuronal subtypes from among the nine possibilities available to Drf-positive neurons. (C, D) Expression of Dac, Cut and *drf* is compared in the larval medulla. Dac (C; magenta) or Cut (D; magenta) and *drf-Gal4 UAS-GFP* (green). (C) Dac expression occurs in a semi-concentric zone with a gap around the dorso-ventral boundary. The Dac domain overlaps the outer sub-domain of the Drf zone.

Figure S5

A.

NP2646 UAS-CD8GFP

Drf

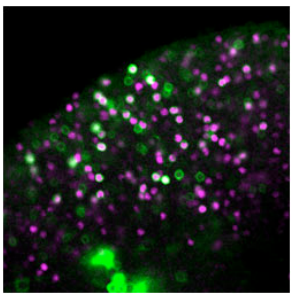

B.

neuronal type	control	drf^{E82}	Drf
Tm27Y	66	0	++
abnormal Tm27Y	0	69	+/-
Tm27	8	0	++
abnormal Tm27	0	9	+/-
Tm5(Y) -like	39	84	-
Tm24(Y) -like	11	16	-
Tm8-like	5	36	-
Tm20-like	5	7	-
$Tm_{3,8}$Y-like	7	19	-
$Tm_{3,6}$-like	5	5	-
Other neurons	2	1	-
Total	148	246	

C.

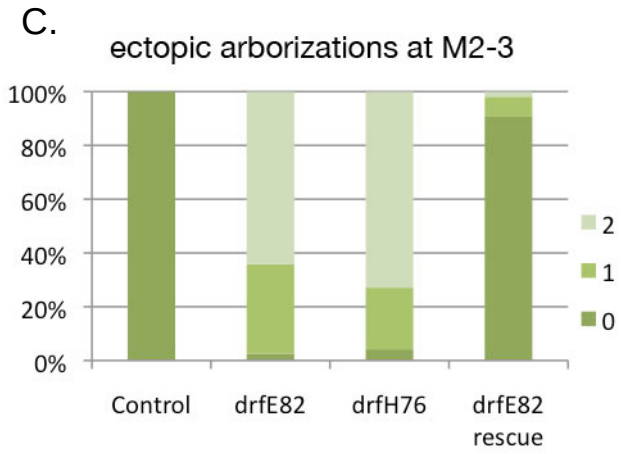

D.

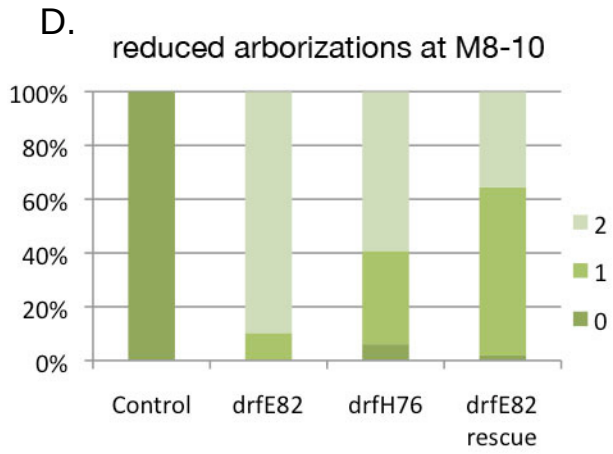

E.

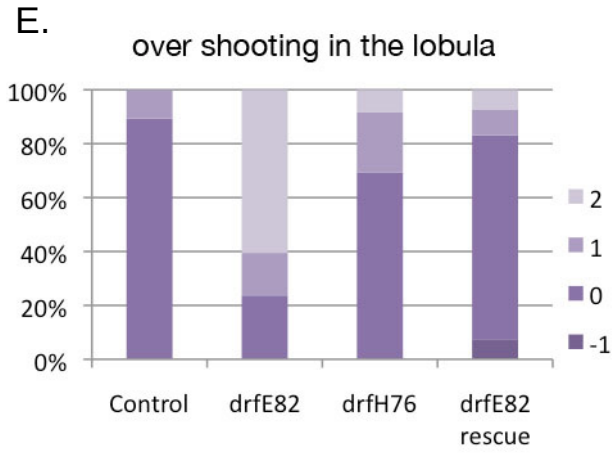

F.

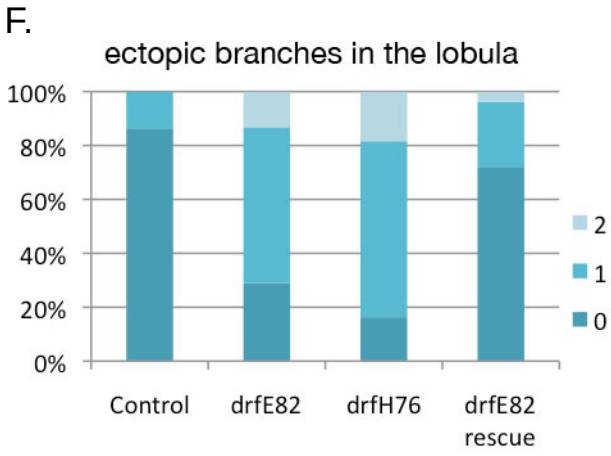

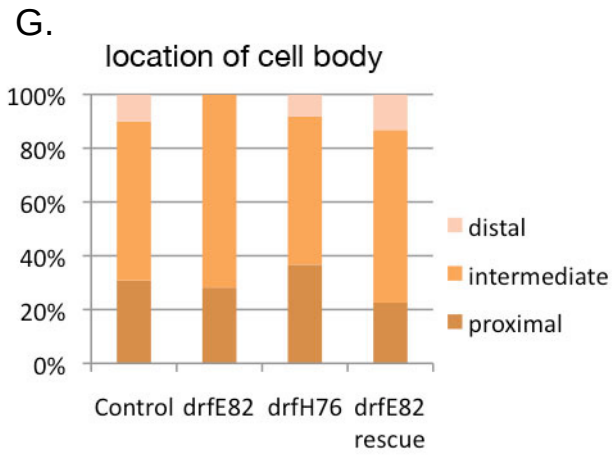

Figure S5. Defects in Tm27(Y) neurons in *drf* mutant clones.

(A) *NP2646 UAS-CD8GFP* expression (green) is found in a subset of Drf-positive neurons (magenta) in the adult medulla cortex. (B) A catalogue of medulla neurons labeled with *NP2646* in wild type and drf^{E82} homozygous clones. Since residual Drf expression is detectable in Tm27(Y) neurons that are homozygous for drf^{E82}, these cells are indeed mutant forms of Tm27(Y). Similar defects were observed in drf^{H76} clones, in which Drf was hardly detectable. Non-Tm27(Y) type neurons were not affected. (C-H) Defects in Tm27Y are quantified in control, drf^{E82}, drf^{H76} homozygous clones and in drf^{E82} homozygous clones rescued by exogenous *drf* expression (n=67, 39, 49 and 53, respectively). (C) Arborizations at M2-3. Class 0: no arborization. Class 1: one fine arborization. Class 2: multiple fine arborizations or one bold arborization. (D) Reduced arborizations at M8-10. Class 0: normal arborizations. Class 1: shortened arborizations throughout M8-10. Class 2: part of axonal shaft at M8-10 completely lacking arborizations. (E) Axonal overshooting in the lobula. Lo4 is defined by reduced NCad signal as indicated by two dotted lines (Fig. 7A2, B2). Class 0: axonal terminals on the first dotted line (Fig. 7A2). Class 1: axonal terminals between the two dotted lines. Class 2: axonal terminals beyond the second dotted line (Fig. 7B2). Class -1: axonal terminals do not reach the first dotted line. (F) Number of ectopic branches in the lobula (Lo1-3). Class 0: no ectopic branch. Class 1: one ectopic branch (Fig. 7B2; arrowhead). Class 2: two or more ectopic branches. (G) Locations of cell bodies. Distal, intermediate and proximal zones are defined as shown in Fig. S4A.

Table S1. Primer list.

Gal4	CAAGGCCTAAA**GGATCC**ATCAAAATGAAGCTACTGTCTTCTATCG
BamHI-AscI	CA**GGCGCGCC**GAACTAGTGGATCTAAACGAG
drfL	CA**CGTACG** TGCAGCTGATGATGATGCCTTCG
BsiWI-BamHI	CA**GGATCC**GGCCATCCCCACCGCTCTGGGGCT3
drfR	CA**GGTACC**GCAATCAGAAATCCAGGAGTCGAAC
KpnI-NotI	CA**GCGGCCGC**GAAACATTATAAACCACGCGCGCC3
hthL	CA**CGTACG**CGCTGGGCTTTAAATTCCCAGAA
BsiWI-BamHI	CA**GGATCC**GTCCATGCCGTAGCCGTGTAGGC
hthR	CA**GGTACC**GCAATACCCGAAGTACACAAACG
KpnI-NotI	CA**GCGGCCGC**ATCAGGAGCTGAAGAAGCAGAAG
bshLz	CAT**CGTACG**GAGGATTACGGCAAGTCCAT
BsiWI-BamHI	CA**GGATCC**GTGGTGGTTGGACCTACGAAGCA
bshRz	CA**GGTACC**ATCACAAGGTGAGTTAATGCTCG
KpnI-NotI	CAT**GCGGCCGC**AACCGCTTTTCCAGACCGGA
Kmr	CATGGCGCGCC**GAATTC**CCTCTAGAAAGCCACGTTGTGTC
AscI-KpnI	CAT**GGTACC**GTCGACCAGTTGGTGATTTTG
bshLB	CAT**GGCGCGCC**GAATGGTCGGCTTTCTCATC
AscI-BamHI	CAT**GGATCC**GGTCGAAGCAATGACAAGTC3
bshRB	CAT**GGATCC**CCCGACTATCAGATACTCGT
BamHI-PacI	CAT**TTAATTAA**AACGCTTGTGACAACGACGA